

# Breaking the Dimensional Barrier: A Pontryagin-Guided Direct Policy Optimization for Continuous-Time Multi-Asset Portfolio

Jeonggyu Huh<sup>1</sup>, Jaegi Jeon<sup>\*2</sup>, and Hyeng Keun Koo<sup>3</sup>

<sup>1</sup>Department of Mathematics, Sungkyunkwan University, Republic of Korea

<sup>2</sup>Graduate School of Data Science, Chonnam National University, Republic of Korea

<sup>3</sup>Department of Financial Engineering, Ajou University, Republic of Korea

April 23, 2025

## Abstract

Solving large-scale, continuous-time portfolio optimization problems involving numerous assets and state-dependent dynamics has long been challenged by the curse of dimensionality. Traditional dynamic programming and PDE-based methods, while rigorous, typically become computationally intractable beyond few state variables ( $\sim 3$ -6 limit in prior studies). To overcome this critical barrier, we introduce the *Pontryagin-Guided Direct Policy Optimization* (PG-DPO) framework. PG-DPO leverages Pontryagin’s Maximum Principle (PMP) and backpropagation-through-time (BPTT) to guide neural network policies, handling exogenous states without dense grids. This PMP-guided approach holds potential for a broad class of sufficiently regular continuous-time control problems. Crucially, our computationally efficient “Two-Stage” variant exploits rapidly stabilizing BPTT costate estimates, converting them into near-optimal Pontryagin controls after only a short warm-up, significantly reducing training overhead. This enables a breakthrough in scalability: numerical experiments show PG-DPO successfully tackles problems with dimensions previously considered far out of reach (up to 50 assets and 10 state variables). The framework delivers near-optimal policies, offering a practical and powerful alternative for high-dimensional continuous-time portfolio choice.

## 1 Introduction

High-dimensional optimal control problems often fall prey to the “curse of dimensionality” (Bellman, 1966), whereby the computational cost of classical dynamic programming (DP) approaches grows exponentially with the number of state variables. In a continuous-time finance setting, this difficulty becomes starkly evident in multi-asset Merton problems (Merton, 1971), where an investor dynamically allocates wealth among numerous risky assets whose drift and volatility may depend on exogenous state variables such as macroeconomic indicators or stochastic volatility factors. While DP or Hamilton–Jacobi–Bellman (HJB) PDE solvers provide a rigorous framework for low-dimensional cases (Bertsekas & Tsitsiklis, 1995), they become intractable as the number of assets or state dimensions increases, with prior influential studies often limited to analyzing problems involving up to approximately 3-5 state variables (Campbell & Viceira, 1999; Lynch, 2001; Balduzzi & Lynch, 1999) or specific frameworks handling around 6 state variables (Garlappi & Skoulakis, 2010), often necessitating simulation-based approaches for tractability (Brandt et al., 2005).

A promising alternative is to employ *Pontryagin’s Maximum Principle (PMP)*, an indirect method that bypasses the explicit computation of value functions (Pontryagin, 2014; Yong & Zhou, 2012)

---

\*Corresponding Author: jaegiyeon@jnu.ac.kr

Rather than storing or approximating a high-dimensional value grid, the PMP characterizes the optimal control in terms of forward–backward differential equations for the state and its *costate* (adjoint). Notably, adding one more state dimension does not produce an exponential explosion in computational requirements, in contrast to DP (Bellman, 1966; Campbell et al., 2003). This makes Pontryagin-based methods appealing for large-scale portfolio optimization problems involving many assets and exogenous state processes (Karatzas et al., 1987).

Recent advances in deep learning further enhance the scalability of methods for solving high-dimensional stochastic control problems (e.g., Han et al., 2018; Raissi et al., 2019, for general PDE-based approaches). Concurrently, deep learning techniques are being applied directly to financial dynamic programming. Some approaches tackle infinite horizon problems via the HJB equation (Duarte et al., 2024), while others aim to directly solve the associated nonlinear PDEs using methods like deep branching algorithms (Nguwi et al., 2024). However, applications such as the Merton HJB have revealed limitations in accuracy or efficiency for certain PDE solvers like Deep BSDE variants (Nguwi et al., 2024). Our PMP-based PG-DPO framework offers a distinct path, naturally handling finite horizons and focusing on the optimality conditions derived from PMP, which are applicable to a wide range of stochastic control problems possessing sufficient regularity. One notable strategy related to the use of adjoint methods in optimal control is to *directly* parameterize the policy (i.e., consumption and investment controls) with neural networks, then apply backpropagation-through-time (BPTT) to enforce Pontryagin’s optimality conditions (Huh, 2024). This strategy, known as “Pontryagin-Guided Direct Policy Optimization (PG-DPO),” circumvents the need to approximate value functions or PDE solutions. Instead, it uses simulation-based gradients that automatically incorporate the adjoint processes, drastically reducing computational overhead in high-dimensional settings (Kushner & Yin, 2003; Borkar & Borkar, 2008).

The purpose of this paper is to develop and implement this PG-DPO framework for the general *multi-asset, state-dependent* continuous-time portfolio problem. We consider an investor who must decide on a continuous consumption rate and an allocation to  $n$  risky assets with state-dependent drift and volatility. By parameterizing the policy with neural networks, we can capture potentially complex relationships dependent on both wealth and the exogenous state. We show how a single forward pass in simulation, coupled with a backward pass via automatic differentiation (BPTT), yields unbiased estimates of the costate processes that PMP requires, guiding the policy towards optimality without the drawbacks of DP. This approach fundamentally relies on the existence and accurate estimation of the costate processes dictated by PMP, applicable whenever the control problem satisfies appropriate regularity conditions allowing for a well-defined Hamiltonian system.

Furthermore, we introduce a “Two-Stage” PG-DPO variant that exploits the observation that costate estimates often stabilize much faster than the full policy network. Once the costates are sufficiently stable (after a short warm-up), one can *bypass* the potentially suboptimal neural policy outputs and directly substitute the costate estimates into the PMP first-order conditions. This recovers a near-optimal control analytically at every time-state point with minimal additional training, significantly reducing computational burden while maintaining high accuracy. This efficiency enables the solution of problems with **dozens of assets and state variables (e.g.,  $n=50$ ,  $k=10$  in our experiments)**, a scale considerably larger than those typically addressed by the numerical methods cited previously. This demonstrated scalability on a benchmarkable problem highlights the potential of leveraging PMP structure via BPTT estimates for tackling other complex, high-dimensional problems that may exhibit similar amenability to costate estimation under suitable regularity conditions.

The main contributions of this paper can be summarized as follows:

- We introduce Pontryagin-Guided Direct Policy Optimization (PG-DPO), featuring a highly efficient “Two-Stage” variant that uses PMP structure and BPTT-derived costates to solve complex continuous-time control problems.

- We demonstrate through numerical experiments the framework’s ability to break the dimensional barrier, successfully tackling portfolio optimization problems with dozens of assets and state factors (up to  $n=50$ ,  $k=10$ ).

In the remainder of this paper, we first present the multi-asset Merton problem with exogenous states in Section 2. Section 3 introduces our Pontryagin-Guided Direct Policy Optimization (PG-DPO) algorithm and its Two-Stage extension. Numerical experiments presented in Section 4 confirm the framework’s scalability and near-optimal performance within this testbed, illustrating its potential for high-dimensional applications. Finally, Section 5 concludes and discusses potential future directions.

## 2 Multi-Asset Continuous-Time Portfolio Problem with State Variables

In this section, we present a multi-asset extension of Merton’s continuous-time portfolio problem (Merton, 1971; Kim & Omberg, 1996; Liu, 2007), allowing the investor to allocate wealth across multiple (potentially correlated) risky assets and a risk-free asset, while consuming continuously. Each risky asset features its own drift and volatility, leading to an  $n$ -dimensional *portfolio weight* vector  $\boldsymbol{\pi}_t$ . Furthermore, an exogenous *state process*  $\mathbf{Y}_t \in \mathbb{R}^k$  influences market parameters such as returns and interest rates, adding additional complexity to the investor’s decision.

Although the wealth  $X_t$  remains scalar, the investor’s optimal policy now depends on both  $\boldsymbol{\pi}_t \in \mathbb{R}^n$  and a high-dimensional state  $\mathbf{Y}_t$ . We handle this through Pontryagin’s maximum principle (Pontryagin, 2014; Yong & Zhou, 2012), introducing a costate for  $X_t$  and another for  $\mathbf{Y}_t$ . Numerically, one can represent  $\{\boldsymbol{\pi}_t, C_t\}$  via neural networks, thereby enabling policy gradient or dynamic programming algorithms even in multi-asset, state-dependent environments.

### 2.1 Problem Formulation with State Variables and Neural Network Controls

Let  $\mathbf{Y}_t \in \mathbb{R}^k$  be a vector of economic state variables that influence the distribution of asset returns. For instance,  $\mathbf{Y}_t$  could include interest rates, macroeconomic indices, volatility factors, etc. We assume each component  $Y_{i,t}$  follows an Ito diffusion:

$$dY_{i,t} = \mu_{Y,i}(t, \mathbf{Y}_t) dt + \sigma_{Y,i}(t, \mathbf{Y}_t) dW_{i,t}^Y, \quad i = 1, \dots, k,$$

with  $\text{Cov}(dW_{i,t}^Y, dW_{j,t}^Y) = \phi_{ij} dt$ . In vector form,

$$d\mathbf{Y}_t = \boldsymbol{\mu}_Y(t, \mathbf{Y}_t) dt + \boldsymbol{\sigma}_Y(t, \mathbf{Y}_t) d\mathbf{W}_t^Y,$$

where  $\boldsymbol{\mu}_Y(t, \mathbf{Y}_t)$  is the  $k \times 1$  drift vector,  $\boldsymbol{\sigma}_Y(t, \mathbf{Y}_t)$  is often assumed to be a  $k \times k$  diagonal matrix of diffusion coefficients, and  $\mathbf{W}_t^Y$  is a  $k \times 1$  vector of potentially correlated Brownian motions driving the state variables.

We consider a financial market with  $n$  risky assets and one risk-free asset. The risk-free asset accumulates wealth at an instantaneous rate  $r(t, \mathbf{Y}_t)$ , which may depend on time and the current state. For  $i = 1, \dots, n$ , the price  $S_{i,t}$  of the  $i$ -th risky asset follows

$$dS_{i,t} = S_{i,t}(\mu_i(t, \mathbf{Y}_t) dt + \sigma_i(t, \mathbf{Y}_t) dW_{i,t}^X).$$

Here,  $\mu_i(t, \mathbf{Y}_t)$  is the instantaneous expected return and  $\sigma_i(t, \mathbf{Y}_t)$  is the instantaneous volatility of asset  $i$ . The  $n$  scalar Brownian motions  $W_{i,t}^X$  may be correlated amongst themselves ( $\text{Cov}(dW_{i,t}^X, dW_{j,t}^X) = \psi_{ij} dt$ ) and with the state variable processes ( $\text{Cov}(dW_{i,t}^X, dW_{j,t}^Y) = \rho_{ij} dt$ ). In vector notation, let  $\boldsymbol{\mu}(t, \mathbf{Y}_t)$  be the  $n \times 1$  vector of expected returns,  $\boldsymbol{\sigma}(t, \mathbf{Y}_t)$  be the  $n \times n$

diagonal matrix of volatilities, and  $\mathbf{W}_t^X$  be the  $n \times 1$  vector of Brownian motions for the risky assets. The risky asset dynamics can be written compactly as

$$d\mathbf{S}_t = \text{diag}(\mathbf{S}_t) \boldsymbol{\mu}(t, \mathbf{Y}_t) dt + \text{diag}(\mathbf{S}_t) \boldsymbol{\sigma}(t, \mathbf{Y}_t) d\mathbf{W}_t^X.$$

Throughout, we work on a complete probability space  $(\Omega, \mathcal{F}, \mathbb{P})$  that carries the  $(n+k)$ -dimensional Brownian motion  $\mathbf{W}_t$  and its natural filtration  $\{\mathcal{F}_t\}_{t \geq 0}$ , augmented to satisfy the *usual conditions* (right-continuity and completeness).

The investor allocates wealth  $X_t$  between the risk-free asset and the  $n$  risky assets. Let  $\boldsymbol{\pi}_t$  be the  $n \times 1$  vector representing the fraction of wealth invested in each risky asset at time  $t$ . The investor also chooses a consumption rate  $C_t$ . The dynamics of the investor's wealth  $X_t$  are governed by the following stochastic differential equation (SDE):

$$dX_t = \left[ X_t \left( r(t, \mathbf{Y}_t) + \boldsymbol{\pi}_t^\top (\boldsymbol{\mu}(t, \mathbf{Y}_t) - r(t, \mathbf{Y}_t) \mathbf{1}) \right) - C_t \right] dt + X_t \boldsymbol{\pi}_t^\top \boldsymbol{\sigma}(t, \mathbf{Y}_t) d\mathbf{W}_t^X. \quad (1)$$

Here,  $\boldsymbol{\mu}(t, \mathbf{Y}_t) - r(t, \mathbf{Y}_t) \mathbf{1}$  represents the vector of instantaneous excess returns over the risk-free rate, and  $\mathbf{1}$  is an  $n \times 1$  vector of ones.

We impose regularity conditions on the market parameters.

**Assumption 1** (Market-parameter regularity). *Fix a finite horizon  $T > 0$ . The coefficients defining the state process  $\mathbf{Y}_t$  and influencing the wealth dynamics  $X_t$  via Eq. (1), namely  $\boldsymbol{\mu}_Y$ ,  $\boldsymbol{\sigma}_Y$ ,  $\boldsymbol{\mu}$ ,  $\boldsymbol{\sigma}$ ,  $r$ , satisfy the following conditions.*

- (a) **Measurability and continuity.** *Each map is jointly Borel-measurable in  $(t, \mathbf{y})$  and continuous in  $\mathbf{y}$  for every fixed  $t \in [0, T]$ .*
- (b) **Global Lipschitz continuity.** *There exists  $K_{\text{Lip}} > 0$  such that for all  $t \in [0, T]$  and  $\mathbf{y}, \mathbf{y}' \in \mathbb{R}^k$ ,*

$$\begin{aligned} & \|\boldsymbol{\mu}_Y(t, \mathbf{y}) - \boldsymbol{\mu}_Y(t, \mathbf{y}')\| + \|\boldsymbol{\sigma}_Y(t, \mathbf{y}) - \boldsymbol{\sigma}_Y(t, \mathbf{y}')\| \\ & + \|\boldsymbol{\mu}(t, \mathbf{y}) - \boldsymbol{\mu}(t, \mathbf{y}')\| + \|\boldsymbol{\sigma}(t, \mathbf{y}) - \boldsymbol{\sigma}(t, \mathbf{y}')\| \leq K_{\text{Lip}} \|\mathbf{y} - \mathbf{y}'\|. \end{aligned}$$

- (c) **Linear growth.** *There exists  $K_{\text{LG}} > 0$  such that for all  $(t, \mathbf{y}) \in [0, T] \times \mathbb{R}^k$ ,*

$$\begin{aligned} & \|\boldsymbol{\mu}_Y(t, \mathbf{y})\|^2 + \|\boldsymbol{\sigma}_Y(t, \mathbf{y})\|^2 + \|\boldsymbol{\mu}(t, \mathbf{y})\|^2 + \|\boldsymbol{\sigma}(t, \mathbf{y})\|^2 \\ & \leq K_{\text{LG}}^2 (1 + \|\mathbf{y}\|^2), \quad |r(t, \mathbf{y})| \leq K_{\text{LG}} (1 + \|\mathbf{y}\|). \end{aligned}$$

Under Assumption 1, the SDE system for  $(\mathbf{Y}_t, X_t)$  (where  $X_t$  depends on the chosen controls  $\boldsymbol{\pi}_t, C_t$ ) admits a unique strong solution for sufficiently well-behaved controls; see Oksendal (2013, Chs. 5-6) for details on existence and uniqueness theorems for SDEs.

We restrict our attention to control processes that are economically sensible and mathematically tractable.

**Assumption 2** (Admissible controls). *A control pair  $(\boldsymbol{\pi}, C)$  is admissible if the following conditions hold:*

- (a) **Adaptedness.**  *$(\boldsymbol{\pi}_t, C_t)_{0 \leq t \leq T}$  is  $\{\mathcal{F}_t\}$ -progressively measurable, where  $\{\mathcal{F}_t\}$  is the filtration generated by the underlying Brownian motions.*
- (b) **Integrability.**

$$\mathbb{E} \int_0^T (\|\boldsymbol{\pi}_t\|^2 + C_t) dt < \infty.$$

- (c) **Boundedness and proportional consumption.** *There exist constants  $\Pi_{\max} > 0$  and  $\xi \in (0, 1)$  such that*

$$\|\boldsymbol{\pi}_t\| \leq \Pi_{\max}, \quad 0 \leq C_t \leq \xi X_t, \quad \forall t \in [0, T] \text{ a.s.}$$

- (d) **Positive wealth.** *The corresponding wealth process  $X_t$  solving (1) remains strictly positive almost surely:*

$$X_t > 0, \quad \forall t \in [0, T].$$

For clarity on the noise structure, we define the combined  $(n + k)$ -dimensional Brownian vector  $\mathbf{W}_t = (\mathbf{W}_t^{X\top}, \mathbf{W}_t^{Y\top})^\top$ . The covariance structure of its increments  $d\mathbf{W}_t$  is given by the matrix  $\boldsymbol{\Omega}$ :

$$\text{Cov}(d\mathbf{W}_t) = \boldsymbol{\Omega} dt = \begin{pmatrix} \Psi & \rho \\ \rho^\top & \Phi \end{pmatrix} dt,$$

where  $\Psi = (\psi_{ij}) \in \mathbb{R}^{n \times n}$  is the covariance matrix of  $d\mathbf{W}_t^X$ ,  $\Phi = (\phi_{ij}) \in \mathbb{R}^{k \times k}$  is the covariance matrix of  $d\mathbf{W}_t^Y$ , and  $\rho = (\rho_{ij}) \in \mathbb{R}^{n \times k}$  is the cross-covariance matrix.

**Assumption 3** (Noise covariance). *The block covariance matrix  $\boldsymbol{\Omega} = \begin{pmatrix} \Psi & \rho \\ \rho^\top & \Phi \end{pmatrix}$  is constant in time and uniformly positive definite: there exists  $\lambda_\Omega > 0$  such that  $z^\top \boldsymbol{\Omega} z \geq \lambda_\Omega \|z\|^2$  for all  $z \in \mathbb{R}^{n+k}$ . (Consequently,  $\Psi$  and  $\Phi$  are individually positive definite and hence invertible.)*

The investor's objective is to choose an admissible control pair  $(\boldsymbol{\pi}, C)$  to maximize the expected discounted utility functional  $J$ :

$$J(\boldsymbol{\pi}, C) = \mathbb{E} \left[ \int_0^T e^{-\delta t} U(C_t) dt + \kappa e^{-\delta T} U(X_T) \right], \quad (2)$$

subject to the wealth dynamics (1) and admissibility constraints (Assumption 2). Here  $\delta > 0$  is the subjective discount rate, and  $\kappa \geq 0$  weights the utility of terminal wealth (bequest motive). The utility function  $U : (0, \infty) \rightarrow \mathbb{R}$  represents the investor's preferences. A widely used specification is the Constant Relative Risk Aversion (CRRA) form:

$$U(x) = \begin{cases} \frac{x^{1-\gamma}}{1-\gamma}, & \gamma > 0, \gamma \neq 1, \\ \ln(x), & \gamma = 1, \end{cases}$$

with  $\gamma > 0$  denoting the coefficient of relative risk aversion (see Pennacchi, 2008).

Assumption 2 (iii) bounds consumption by  $C_t \leq \xi X_t$  with  $\xi \in (0, 1)$ , while Assumption 4 (b) gives a  $C^2$ , strictly concave utility  $U$  satisfying the Inada limits. Because  $\delta > 0$  and  $X_t > 0$  a.s. (Assumption 2 (iv)), we have

$$\mathbb{E}[e^{-\delta t} U(C_t)] \leq e^{-\delta t} U(\xi \mathbb{E}[X_t]) < \infty, \quad \forall t \in [0, T],$$

and similarly  $\mathbb{E}[U(X_T)] < \infty$ . Hence the functional  $J(\boldsymbol{\pi}, C)$  in (2) is finite for every admissible control pair, so the value function  $V$  is well defined.

The value function  $V(t, x, \mathbf{y})$  associated with this problem represents the maximum expected utility achievable starting from wealth  $x$  and state  $\mathbf{y}$  at time  $t$ . Formally,

$$V(t, x, \mathbf{y}) = \sup_{(\boldsymbol{\pi}_s, C_s)_{s \in [t, T]}} \mathbb{E}_{t, x, \mathbf{y}} \left[ \int_t^T e^{-\delta(s-t)} U(C_s) ds + \kappa e^{-\delta(T-t)} U(X_T) \right],$$

where the supremum is taken over all admissible control processes on  $[t, T]$ , and  $\mathbb{E}_{t, x, \mathbf{y}}[\cdot] = \mathbb{E}[\cdot | X_t = x, \mathbf{Y}_t = \mathbf{y}]$  denotes the conditional expectation.

Additional assumptions are needed for the well-posedness of the problem and regularity of the value function.

**Assumption 4** (Uniform non-degeneracy and utility).

- (a) **Uniform non-degeneracy of risky-asset volatility.** Let  $a(t, \mathbf{y}) := \boldsymbol{\sigma}(t, \mathbf{y}) \Psi \boldsymbol{\sigma}(t, \mathbf{y})^\top$  be the instantaneous covariance matrix of the risky asset returns (Note: original used  $\boldsymbol{\sigma}\boldsymbol{\sigma}^\top$ , assuming  $\Psi = I$ ; using  $\boldsymbol{\sigma}\Psi\boldsymbol{\sigma}^\top$  is more general if  $\mathbf{W}^X$  components are correlated and  $\boldsymbol{\sigma}$  is diagonal). We assume there exists  $\lambda > 0$  such that

$$\mathbf{z}^\top a(t, \mathbf{y}) \mathbf{z} \geq \lambda \|\mathbf{z}\|^2, \quad \forall (t, \mathbf{y}, \mathbf{z}) \in [0, T] \times \mathbb{R}^k \times \mathbb{R}^n.$$

(Equivalently, the covariance matrix of risky returns  $a(t, \mathbf{y})$  is uniformly positive definite, ensuring invertibility, which is crucial for solving the portfolio problem.)

- (b) **Utility specification.** The utility function  $U : (0, \infty) \rightarrow \mathbb{R}$  satisfies  $U \in C^2(0, \infty)$ ,  $U' > 0$ ,  $U'' < 0$  (strictly increasing and concave), and the Inada conditions  $\lim_{c \downarrow 0} U'(c) = \infty$ ,  $\lim_{c \uparrow \infty} U'(c) = 0$ .
- (c) **Discount and bequest parameters.** The subjective discount rate satisfies  $\delta > 0$  and the terminal weight satisfies  $\kappa \geq 0$ .

Assumption 4 (a) guarantees the diffusion related to risky assets is non-degenerate, a key ingredient for the regularity of the associated Hamilton-Jacobi-Bellman (HJB) PDE. Parts (b)-(c) ensure the objective functional is well-defined and satisfies standard preference assumptions. Combined with the coefficient regularity in Assumption 1, these conditions typically yield the existence, uniqueness, and sufficient smoothness (e.g.,  $V \in C^{1,2,2}$ ) of the solution to the HJB equation, allowing for verification theorems to be applied; see Oksendal (2013, Chs. 6-7) and related literature on optimal portfolio choice.

In our numerical approach, we parameterize the control policies using neural networks (NNs). The portfolio allocation  $\boldsymbol{\pi}_t$  and consumption rate  $C_t$  are represented as functions of the current time  $t$ , wealth  $X_t$ , and state  $\mathbf{Y}_t$ , determined by the NN parameters  $\theta$  and  $\phi$ :

$$\boldsymbol{\pi}_t = \boldsymbol{\pi}_\theta(t, X_t, \mathbf{Y}_t), \quad C_t = C_\phi(t, X_t, \mathbf{Y}_t).$$

These parameters  $\theta$  and  $\phi$  are then optimized to maximize the objective  $J$ .

## 2.2 Optimality Conditions via Pontryagin's Maximum Principle

We now apply Pontryagin's Maximum Principle (PMP) to the continuous-time portfolio problem formulated in Section 2.1, where market parameters depend on the exogenous state process  $\{\mathbf{Y}_t\}_{0 \leq t \leq T}$ . PMP provides necessary conditions for optimality through a system of forward-backward stochastic differential equations (FBSDEs), which couple the dynamics of the state variables with those of associated costate variables.

The system state includes the investor's wealth  $X_t$  and the exogenous state variables  $\mathbf{Y}_t \in \mathbb{R}^k$ . The corresponding costate processes represent the sensitivity of the value function  $V$  to changes in the state:  $\lambda_t = V_x(t, X_t, \mathbf{Y}_t)$  is the scalar costate for wealth (marginal value of wealth), and  $\boldsymbol{\eta}_t = V_y(t, X_t, \mathbf{Y}_t)$  is the  $k$ -dimensional costate vector for the exogenous state variables (marginal value of state variables).

Under an optimal control policy  $(\boldsymbol{\pi}_t^*, C_t^*)$ , the evolution of the system state, comprising the wealth process  $X_t^*$  and the exogenous variables  $\mathbf{Y}_t$ , is described by the following forward stochastic differential equations:

$$\begin{aligned} dX_t^* &= \left[ X_t^* \left( r(t, \mathbf{Y}_t) + \boldsymbol{\pi}_t^{*\top} (\boldsymbol{\mu}(t, \mathbf{Y}_t) - r(t, \mathbf{Y}_t) \mathbf{1}) \right) - C_t^* \right] dt \\ &\quad + X_t^* \boldsymbol{\pi}_t^{*\top} \boldsymbol{\sigma}(t, \mathbf{Y}_t) d\mathbf{W}_t^X, \end{aligned} \tag{3}$$

$$d\mathbf{Y}_t = \boldsymbol{\mu}_Y(t, \mathbf{Y}_t) dt + \boldsymbol{\sigma}_Y(t, \mathbf{Y}_t) d\mathbf{W}_t^Y, \tag{4}$$

with initial conditions  $X_0^* = x_0 > 0$  and  $\mathbf{Y}_0 = \mathbf{y}_0 \in \mathbb{R}^k$ . Recall the definitions of the volatility matrix  $\boldsymbol{\sigma}(t, \mathbf{Y}_t)$  and the covariance structure  $\boldsymbol{\Omega}$  of the combined Brownian motion  $\mathbf{W}_t = (\mathbf{W}_t^{X^\top}, \mathbf{W}_t^{Y^\top})^\top$ .

Complementing these forward dynamics, the optimal costate processes  $(\lambda_t^*, \boldsymbol{\eta}_t^*)$  satisfy a system of backward stochastic differential equations (BSDEs). These equations are driven by derivatives of the Hamiltonian  $\mathcal{H}$  associated with the control problem:

$$-d\lambda_t^* = \mathcal{H}_x(t, X_t^*, \mathbf{Y}_t, \boldsymbol{\pi}_t^*, C_t^*, \lambda_t^*, \boldsymbol{\eta}_t^*, \mathbf{Z}_t) dt - \mathbf{Z}_t^{\lambda X} d\mathbf{W}_t^X - \mathbf{Z}_t^{\lambda Y} d\mathbf{W}_t^Y, \quad (5)$$

$$-d\boldsymbol{\eta}_t^* = \mathcal{H}_y(t, X_t^*, \mathbf{Y}_t, \boldsymbol{\pi}_t^*, C_t^*, \lambda_t^*, \boldsymbol{\eta}_t^*, \mathbf{Z}_t) dt - \mathbf{Z}_t^{\eta X} d\mathbf{W}_t^X - \mathbf{Z}_t^{\eta Y} d\mathbf{W}_t^Y. \quad (6)$$

Here,  $\mathcal{H}_x = \partial\mathcal{H}/\partial x$  and  $\mathcal{H}_y = \nabla_y \mathcal{H}$  represent the partial derivatives of the Hamiltonian. The terms  $\mathbf{Z}_t^{\lambda X} \in \mathbb{R}^{1 \times n}$ ,  $\mathbf{Z}_t^{\lambda Y} \in \mathbb{R}^{1 \times k}$ ,  $\mathbf{Z}_t^{\eta X} \in \mathbb{R}^{k \times n}$ , and  $\mathbf{Z}_t^{\eta Y} \in \mathbb{R}^{k \times k}$  are adapted processes arising from the martingale representation theorem applied to the costates, collectively denoted by  $\mathbf{Z}_t$ . The derivatives  $\mathcal{H}_x, \mathcal{H}_y$  generally depend on the state, costate, controls, and the  $\mathbf{Z}_t$  terms themselves, reflecting the system's interconnectedness through the value function's second-order derivatives. The terminal conditions are determined by the objective functional:  $\lambda_T^* = \kappa e^{-\delta T} U'(X_T^*)$  and  $\boldsymbol{\eta}_T^* = \mathbf{0}$ .

The application of PMP involves maximizing a Hamiltonian function. To properly account for the dependence of the wealth diffusion on the control  $\boldsymbol{\pi}$ , the Hamiltonian should incorporate the interaction between the costate dynamics (represented by  $\mathbf{Z}$  terms) and the diffusion coefficients. Following formulations in stochastic control theory (e.g., Yong & Zhou, 2012), the appropriate Hamiltonian  $\mathcal{H}$  can be expressed as:

$$\begin{aligned} \mathcal{H}(t, x, \mathbf{y}, \boldsymbol{\pi}, C, \lambda, \boldsymbol{\eta}, \mathbf{Z}^{\lambda X}, \mathbf{Z}^{\lambda Y}, \mathbf{Z}^{\eta X}, \mathbf{Z}^{\eta Y}) \\ = e^{-\delta t} U(C) + \lambda \left[ x(r(t, \mathbf{y}) + \boldsymbol{\pi}^\top (\boldsymbol{\mu}(t, \mathbf{y}) - r(t, \mathbf{y})\mathbf{1})) - C \right] + \boldsymbol{\eta}^\top \boldsymbol{\mu}_Y(t, \mathbf{y}) \\ + \mathbf{Z}^{\lambda X} (x \boldsymbol{\sigma}(t, \mathbf{y})^\top \boldsymbol{\pi}) + \text{Tr}(\mathbf{Z}^{\eta Y \top} \boldsymbol{\sigma}_Y(t, \mathbf{y})) + \dots \end{aligned} \quad (7)$$

For clarity in deriving the FOC for  $\boldsymbol{\pi}$ , the crucial term involving  $\boldsymbol{\pi}$  beyond the drift component is the one coupling  $\mathbf{Z}^{\lambda X}$  with the wealth diffusion  $x \boldsymbol{\pi}^\top \boldsymbol{\sigma}(t, \mathbf{Y}_t)$  originating from  $d\mathbf{W}_t^X$ . We focus on these terms for the maximization step.

To ensure the well-posedness of this FBSDE system and the applicability of PMP, additional smoothness conditions on the model coefficients are typically required.

**Assumption 5** (Additional regularity for PMP). *In addition to Assumptions 1, 2, and 4, we assume:*

- (a)  **$C^1$ -regular coefficients w.r.t.  $\mathbf{y}$ .** *All coefficient functions  $\boldsymbol{\mu}_Y, \boldsymbol{\sigma}_Y, \boldsymbol{\mu}, \boldsymbol{\sigma}, r$  are continuously differentiable with respect to the state vector  $\mathbf{y}$ . Furthermore, their partial derivatives  $(\partial_y f)$  are globally Lipschitz continuous in  $\mathbf{y}$  and satisfy linear growth conditions. This ensures that the drift terms in the costate BSDEs, involving derivatives like  $\mathcal{H}_y$ , satisfy the required regularity conditions for the existence and uniqueness of solutions (cf. Yong & Zhou, 2012).*

The core requirement of Pontryagin's Maximum Principle is that the optimal controls  $(\boldsymbol{\pi}_t^*, C_t^*)$  must maximize the Hamiltonian  $\mathcal{H}$  (7) pointwise in time, almost surely, given the optimal state and costate processes  $(X_t^*, \mathbf{Y}_t, \lambda_t^*, \boldsymbol{\eta}_t^*, \mathbf{Z}_t^*)$ . Assuming interior solutions allows us to derive the first-order conditions (FOCs) for optimality. Maximization with respect to the consumption rate  $C_t$  yields the standard condition:

$$e^{-\delta t} U'(C_t^*) = \lambda_t^*. \quad (8)$$

This classic result links optimal consumption  $C_t^* = (U')^{-1}(e^{\delta t} \lambda_t^*)$  inversely to the marginal value of wealth  $\lambda_t^*$ . Maximization with respect to the portfolio weights  $\boldsymbol{\pi}_t$  requires differentiating

$\mathcal{H}$  with respect to  $\boldsymbol{\pi}$ , including the term involving  $\mathbf{Z}^{\lambda X}$ . From (7), the relevant terms are  $\lambda x \boldsymbol{\pi}^\top (\boldsymbol{\mu} - r \mathbf{1})$  and  $\mathbf{Z}^{\lambda X} (x \boldsymbol{\sigma}^\top \boldsymbol{\pi})$ . Setting the gradient  $\nabla_{\boldsymbol{\pi}} \mathcal{H} = \mathbf{0}$  gives (assuming  $X_t^* > 0$ ):

$$\lambda_t^* X_t^* (\boldsymbol{\mu}(t, \mathbf{Y}_t) - r(t, \mathbf{Y}_t) \mathbf{1}) + X_t^* \boldsymbol{\sigma}(t, \mathbf{Y}_t) (\mathbf{Z}_t^{\lambda X^*})^\top = \mathbf{0}.$$

Dividing by  $X_t^*$ , we obtain the FOC for the optimal portfolio:

$$\lambda_t^* (\boldsymbol{\mu}(t, \mathbf{Y}_t) - r(t, \mathbf{Y}_t) \mathbf{1}) + \boldsymbol{\sigma}(t, \mathbf{Y}_t) (\mathbf{Z}_t^{\lambda X^*})^\top = \mathbf{0}. \quad (9)$$

This first-order condition implicitly defines the optimal portfolio  $\boldsymbol{\pi}_t^*$  through its dependence on the costate  $\lambda_t^*$  and the martingale component  $\mathbf{Z}_t^{\lambda X^*}$ .

To obtain an explicit expression for  $\boldsymbol{\pi}_t^*$ , we need to relate the martingale component  $\mathbf{Z}^{\lambda X^*}$  to the derivatives of the value function. Applying Ito's lemma to  $\lambda_t = V_x(t, X_t, \mathbf{Y}_t)$  and matching terms with the BSDE (5) establishes this relationship (the precise derivation often involves careful application of Ito's formula for processes driven by correlated Brownian motions, see e.g., standard texts or appendices like Appendix A). This procedure yields an expression for  $\mathbf{Z}^{\lambda X^*}$  in terms of  $V_{xx}$ ,  $V_{xy}$ , the optimal controls  $\boldsymbol{\pi}_t^*$ , and the model parameters  $(\boldsymbol{\sigma}, \boldsymbol{\sigma}_Y, \Psi, \rho)$ . Substituting this expression into the FOC (9) and solving the resulting algebraic equation for  $\boldsymbol{\pi}_t^*$  leads to the well-known optimal portfolio formula:

$$\begin{aligned} \boldsymbol{\pi}_t^* = & -\frac{V_x}{X_t V_{xx}} \Sigma^{-1}(t, \mathbf{Y}_t) (\boldsymbol{\mu}(t, \mathbf{Y}_t) - r(t, \mathbf{Y}_t) \mathbf{1}) \\ & - \frac{V_{xy}}{X_t V_{xx}} \Sigma^{-1}(t, \mathbf{Y}_t) \boldsymbol{\sigma}(t, \mathbf{Y}_t) \rho \boldsymbol{\sigma}_Y^\top(t, \mathbf{Y}_t). \end{aligned} \quad (10)$$

Here,  $\Sigma(t, \mathbf{Y}_t) = \boldsymbol{\sigma}(t, \mathbf{Y}_t) \Psi \boldsymbol{\sigma}(t, \mathbf{Y}_t)^\top$  represents the instantaneous covariance matrix of the risky asset returns. The value function derivatives  $V_x = \lambda_t^*$ ,  $V_{xx} = \partial_x \lambda_t^*$ , and  $V_{xy} = \partial_{\mathbf{y}} \lambda_t^*$  are evaluated along the optimal path  $(t, X_t^*, \mathbf{Y}_t)$ . The formula clearly separates the portfolio into two components: the *myopic demand*, which optimizes the immediate risk-return trade-off as if the investment opportunity set were constant, and the *intertemporal hedging demand*, which adjusts the portfolio to mitigate risks arising from future stochastic changes in the state variables  $\mathbf{Y}_t$ . The hedging demand's magnitude and direction depend on the correlation  $\rho$  between asset returns and state variable innovations, and crucially on  $V_{xy}$ , which measures how the marginal value of wealth changes with the state variables.

For illustration, in the simplified case with one risky asset ( $n = 1$ ) and one state variable ( $k = 1$ ), the optimal allocation (10) becomes:

$$\pi_t^* = -\frac{V_x}{X_t V_{xx} \sigma^2} (\mu(t, Y_t) - r(t, Y_t)) - \frac{V_{xy}}{X_t V_{xx} \sigma^2} \sigma \rho \sigma_Y,$$

clearly showing the separation between the myopic component, proportional to the market price of risk, and the hedging component, proportional to  $V_{xy}$  and the correlation  $\rho$ .

## 2.3 Applications to Financial Models

### 2.3.1 A Multi-Asset Model with One OU Factor

We first consider a model with  $n$  risky assets whose risk premia are driven by a single Ornstein–Uhlenbeck (OU) factor. Specifically, each asset  $i$  has a constant volatility  $\sigma_i > 0$  and a time-varying risk premium proportional to an OU state variable  $Y_t$ , such that the expected return is  $r + \alpha_i \sigma_i Y_t$ , where  $r$  is the constant risk-free rate and  $\alpha_i$  is a loading coefficient. The state variable  $Y_t$  follows the OU process:

$$dY_t = \kappa_Y (\theta_Y - Y_t) dt + \sigma_Y dW_t^Y,$$

where  $\kappa_Y > 0$  is the mean-reversion speed,  $\theta_Y \in \mathbb{R}$  is the long-term mean, and  $\sigma_Y > 0$  is the factor volatility. The Brownian motion  $W_t^Y$  may be correlated with the asset return processes.

The price dynamics for the  $i$ -th risky asset,  $S_{i,t}$ , are given by:

$$\frac{dS_{i,t}}{S_{i,t}} = (r + \alpha_i \sigma_i Y_t) dt + \sigma_i dW_{i,t}^S.$$

The Brownian motions driving the assets,  $\mathbf{W}_t^S = (W_{1,t}^S, \dots, W_{n,t}^S)^\top$ , have an  $n \times n$  covariance matrix  $\Psi dt$ , i.e.,  $\text{Cov}(d\mathbf{W}_t^S) = \Psi dt$ . Furthermore, each  $dW_{i,t}^S$  may have a correlation  $\rho_i$  with  $dW_t^Y$ ; let  $\boldsymbol{\rho} = (\rho_1, \dots, \rho_n)^\top$ .

Let  $X_t$  denote total wealth. The investor chooses a consumption rate  $C_t \geq 0$  and portfolio weights  $\boldsymbol{\pi}_t \in \mathbb{R}^n$  for the risky assets. The wealth dynamics follow:

$$dX_t = \left[ X_t \left( \left(1 - \boldsymbol{\pi}_t^\top \mathbf{1}\right) r + \boldsymbol{\pi}_t^\top (r\mathbf{1} + \boldsymbol{\alpha}\boldsymbol{\sigma}Y_t) \right) - C_t \right] dt + X_t \boldsymbol{\pi}_t^\top \text{diag}(\boldsymbol{\sigma}) d\mathbf{W}_t^S,$$

where  $\boldsymbol{\alpha} = (\alpha_1, \dots, \alpha_n)^\top$ , and  $\boldsymbol{\sigma} = (\sigma_1, \dots, \sigma_n)^\top$ . The instantaneous covariance matrix of the  $n$ -asset returns is  $\Sigma = \text{diag}(\boldsymbol{\sigma}) \Psi \text{diag}(\boldsymbol{\sigma})$ .

For an investor with CRRA utility  $U(x)$  and discount rate  $\delta > 0$ , the optimal consumption  $C_t^*$  is determined by  $C_t^* = (U')^{-1}(e^{\delta t} \lambda_t^*)$ , where  $\lambda_t^*$  is the costate associated with wealth  $X_t$ . The PMP first-order condition yields the optimal portfolio  $\boldsymbol{\pi}_t^* \in \mathbb{R}^n$  as:

$$\boldsymbol{\pi}_t^* = -\frac{1}{X_t^* (\partial_x \lambda_t^*)} \Sigma^{-1} \{ \lambda_t^* (\boldsymbol{\alpha}\boldsymbol{\sigma}) Y_t + (\partial_Y \lambda_t^*) \sigma_Y (\boldsymbol{\sigma}\boldsymbol{\rho}) \}.$$

This expression involves the costate  $\lambda_t^*$  and its derivatives  $\partial_x \lambda_t^*$  and  $\partial_Y \lambda_t^*$ . The first term within the braces represents the myopic demand driven by the risk premium  $(\boldsymbol{\alpha}\boldsymbol{\sigma})Y_t$ , and the second term captures the intertemporal hedging demand arising from the state variable  $Y_t$ . If  $n = 1$ , this simplifies to  $\pi_t^* = -\frac{1}{\sigma^2 X_t^* \partial_x \lambda_t^*} \{ \lambda_t^* \alpha \sigma Y_t + \sigma (\partial_Y \lambda_t^*) \sigma_Y \rho \}$ . For the specific case without intermediate consumption ( $C_t = 0$ ), an analytic solution involving Riccati ODEs can be derived using the HJB framework (Kim & Omberg, 1996), as detailed in Appendix B.1.

### 2.3.2 A Multi-Asset, Multi-Factor Model

We then extend this setup to a more general *multi-factor* environment, considering  $n$  risky assets whose risk premia are driven by a  $k$ -dimensional OU factor vector  $\mathbf{Y}_t \in \mathbb{R}^k$ . The risk premium for asset  $i = 1, \dots, n$  is  $\sigma_i (\boldsymbol{\alpha}_i^\top \mathbf{Y}_t)$ , where  $\boldsymbol{\alpha}_i \in \mathbb{R}^k$  contains the factor loadings for asset  $i$ . The volatility  $\sigma_i$  for asset  $i$  is constant. This allows for richer interactions between multiple risk sources and asset returns.

The factor vector  $\mathbf{Y}_t \in \mathbb{R}^k$  follows a multivariate OU process:

$$d\mathbf{Y}_t = \kappa_Y (\boldsymbol{\theta}_Y - \mathbf{Y}_t) dt + \boldsymbol{\sigma}_Y d\mathbf{W}_t^Y,$$

where  $\kappa_Y \in \mathbb{R}^{k \times k}$  is a mean-reversion matrix,  $\boldsymbol{\theta}_Y \in \mathbb{R}^k$  is the long-run mean vector, and  $\boldsymbol{\sigma}_Y \in \mathbb{R}^{k \times k}$  governs the factor volatilities and correlations (e.g.,  $\text{Cov}(d\mathbf{W}_t^Y) = \Phi dt$ ).

The  $n$  risky assets, with prices  $S_t^i$ , follow:

$$\frac{dS_t^i}{S_t^i} = \left( r + \sigma_i \boldsymbol{\alpha}_i^\top \mathbf{Y}_t \right) dt + \sigma_i dW_t^{X,i}, \quad i = 1, \dots, n.$$

Here,  $\mathbf{W}_t^X \in \mathbb{R}^n$  is a Brownian motion with covariance matrix  $\Psi dt$ . The asset shocks  $\mathbf{W}_t^X$  and factor shocks  $\mathbf{W}_t^Y$  can be correlated, with  $\text{Cov}(dW_t^{X,i}, dW_t^{Y,j}) = \rho_{ij} dt$ . Let  $\rho \in \mathbb{R}^{n \times k}$  be the matrix of cross-correlations.

With portfolio weights  $\boldsymbol{\pi}_t = (\pi_t^1, \dots, \pi_t^n)^\top$  and consumption  $C_t$ , wealth  $X_t$  evolves as:

$$dX_t = \left[ X_t \left( r + \sum_{i=1}^n \pi_t^i \sigma_i (\boldsymbol{\alpha}_i^\top \mathbf{Y}_t) \right) - C_t \right] dt + X_t \sum_{i=1}^n \pi_t^i \sigma_i dW_t^{X,i}.$$

For CRRA utility with discount  $\delta$ , the optimal consumption  $C_t^*$  depends on the wealth costate  $\lambda_t^*$ . The optimal portfolio  $\boldsymbol{\pi}_t^* \in \mathbb{R}^n$  is given by the PMP first-order condition (Eq. (10)), which in this context becomes:

$$\boldsymbol{\pi}_t^* = - \frac{1}{X_t^* (\partial_x \lambda_t^*)} \Sigma^{-1} \left\{ \underbrace{\lambda_t^* \text{diag}(\boldsymbol{\sigma}) \mathbf{A} \mathbf{Y}_t}_{\text{Myopic Term}} + \underbrace{\text{diag}(\boldsymbol{\sigma}) \rho \boldsymbol{\sigma}_Y (\partial_{\mathbf{Y}} \lambda_t^*)^\top}_{\text{Hedging Term}} \right\},$$

where  $\boldsymbol{\sigma} = (\sigma_1, \dots, \sigma_n)^\top$ ,  $\Sigma = \text{diag}(\boldsymbol{\sigma}) \Psi \text{diag}(\boldsymbol{\sigma})$  is the  $n \times n$  asset return covariance,  $\mathbf{A} = (\boldsymbol{\alpha}_1, \dots, \boldsymbol{\alpha}_n)^\top$  is the  $n \times k$  matrix of factor loadings, and  $\partial_{\mathbf{Y}} \lambda_t^*$  is the  $k \times 1$  gradient vector of the costate with respect to the factors  $\mathbf{Y}_t$ . This explicitly separates the demand into a myopic part driven by the current expected excess returns ( $\text{diag}(\boldsymbol{\sigma}) \mathbf{A} \mathbf{Y}_t$ ) and a hedging part driven by the sensitivity to factor changes ( $\partial_{\mathbf{Y}} \lambda_t^*$ ) and their correlations ( $\rho, \Psi, \Phi$ ).

Similar to the single-factor case, an analytic solution for the terminal wealth problem ( $C_t = 0$ ) with CRRA utility can often be found using an exponential-quadratic value function ansatz, leading to matrix Riccati ODEs. Details are presented in Appendix B.2.

### 3 A Gradient-Based Algorithm for Multi-Asset Policy Optimization

While Pontryagin's Maximum Principle (PMP) provides necessary optimality conditions via forward-backward stochastic differential equations (FBSDEs, Section 2.2), solving these analytically is often infeasible in high dimensions. We therefore adopt a *gradient-based* numerical approach using deep learning. The core idea is to parameterize the investor's policy  $(\boldsymbol{\pi}_t, C_t)$  with neural networks  $(\boldsymbol{\pi}_\theta(t, x, \mathbf{y}), C_\phi(t, x, \mathbf{y}))$ , where  $(\theta, \phi)$  are the parameters to be optimized.

The objective is to find parameters  $(\theta, \phi)$  that maximize the expected utility achieved by the policy  $(\boldsymbol{\pi}_\theta, C_\phi)$ . To ensure robustness across different starting scenarios, we aim to maximize the **extended value function**,  $\tilde{J}(\theta, \phi)$ . This is defined as the expected value of the conditional expected utility  $J(t_0, x_0, \mathbf{y}_0; \theta, \phi)$  achieved under policy  $(\theta, \phi)$ , where the initial state  $(t_0, x_0, \mathbf{y}_0)$  is drawn from a distribution  $\eta$  over a relevant domain  $\mathcal{D}$ :

$$J(t_0, x_0, \mathbf{y}_0; \theta, \phi) = \mathbb{E}^{\theta, \phi} \left[ \int_{t_0}^T e^{-\delta(u-t_0)} U(C_\phi(u, X_u, \mathbf{Y}_u)) du + \kappa e^{-\delta(T-t_0)} U(X_T) \mid X_{t_0} = x_0, \mathbf{Y}_{t_0} = \mathbf{y}_0 \right] \quad (11)$$

$$\tilde{J}(\theta, \phi) = \mathbb{E}_{(t_0, x_0, \mathbf{y}_0) \sim \eta} [J(t_0, x_0, \mathbf{y}_0; \theta, \phi)] \quad (12)$$

Here,  $\mathbb{E}^{\theta, \phi}[\cdot]$  denotes expectation under the dynamics generated by policy  $(\theta, \phi)$ .

This paper develops and implements the *Pontryagin-Guided Direct Policy Optimization (PG-DPO)* framework to maximize  $\tilde{J}(\theta, \phi)$ . PG-DPO leverages automatic differentiation, specifically backpropagation-through-time (BPTT), applied to Monte Carlo simulations drawn from the initial state distribution  $\eta$ . A key feature is that BPTT applied to these simulations yields not only unbiased estimates of the policy gradient  $\nabla \tilde{J}$  needed for optimization, but also inherently calculates estimates of the Pontryagin costate variables  $(\lambda_k^{(i)}, \boldsymbol{\eta}_k^{(i)})$  along each path, representing sensitivities dictated by PMP.

This dual output enables distinct algorithmic approaches detailed in the subsequent subsections.

### 3.1 Baseline PG-DPO for the Extended Objective

The baseline PG-DPO algorithm aims to maximize the extended value function  $\tilde{J}(\theta, \phi)$  (defined in Eq. (12)) using mini-batch stochastic gradient ascent. The core idea is to approximate the gradient  $\nabla \tilde{J}$  by averaging gradients computed on individual sample paths, where each path starts from a randomly drawn initial state. Each iteration  $j$  of the algorithm involves the following steps:

1. **Sample Initial States:** Draw a mini-batch of  $M$  initial states  $\{(t_0^{(i)}, x_0^{(i)}, \mathbf{y}_0^{(i)})\}_{i=1}^M$  from the distribution  $\eta$  over the domain  $\mathcal{D}$ .
2. **Simulate Forward Paths:** For each sampled initial state  $i$ , simulate a discrete-time trajectory  $\{(X_k^{(i)}, \mathbf{Y}_k^{(i)})\}_{k=0}^N$  forward from  $t_k = t_0^{(i)}$  to  $t_N = T$ , using the current policy networks  $(\pi_\theta, C_\phi)$  and correctly correlated Brownian increments  $(\Delta \mathbf{W}_k^{(i),X}, \Delta \mathbf{W}_k^{(i),Y})$  derived from the Cholesky factor  $L$  of  $\Sigma_{\text{block}}$ . The state evolution follows:

$$\begin{aligned} \mathbf{Y}_{k+1}^{(i)} &= \mathbf{Y}_k^{(i)} + \boldsymbol{\mu}_Y(t_k^{(i)}, \mathbf{Y}_k^{(i)})\Delta t^{(i)} + \boldsymbol{\sigma}_Y(t_k^{(i)}, \mathbf{Y}_k^{(i)})\Delta \mathbf{W}_k^{(i),Y}, \\ X_{k+1}^{(i)} &= X_k^{(i)} + \left[ X_k^{(i)} \left( (1 - \boldsymbol{\pi}_k^{(i)\top} \mathbf{1})r(t_k^{(i)}, \mathbf{Y}_k^{(i)}) + \boldsymbol{\pi}_k^{(i)\top} \boldsymbol{\mu}(t_k^{(i)}, \mathbf{Y}_k^{(i)}) \right) - C_k^{(i)} \right] \Delta t^{(i)} \\ &\quad + X_k^{(i)} \boldsymbol{\pi}_k^{(i)\top} \boldsymbol{\sigma}(t_k^{(i)}, \mathbf{Y}_k^{(i)})\Delta \mathbf{W}_k^{(i),X}, \end{aligned}$$

where  $\Delta t^{(i)} = (T - t_0^{(i)})/N$ .

3. **Calculate Realized Reward per Path:** For each path  $i$ , compute the realized cumulative reward, explicitly noting its dependence on the starting state and policy parameters, denoted as  $J^{(i)}(t_0^{(i)}, x_0^{(i)}, \mathbf{y}_0^{(i)}; \theta, \phi)$ :

$$J^{(i)}(t_0^{(i)}, x_0^{(i)}, \mathbf{y}_0^{(i)}; \theta, \phi) = \sum_{k=0}^{N-1} e^{-\delta t_k^{(i)}} U(C_\phi(t_k^{(i)}, X_k^{(i)}, \mathbf{Y}_k^{(i)}))\Delta t^{(i)} + \kappa e^{-\delta T} U(X_N^{(i)}).$$

This value  $J^{(i)}(t_0^{(i)}, \dots)$  is a stochastic sample related to the conditional expected utility  $J(t_0^{(i)}, \dots)$  defined in Eq. (11).

4. **Apply BPTT for Policy Gradient Estimate:** Treat the simulation process for path  $i$  as a computational graph. Apply automatic differentiation (BPTT) to compute the gradient of the realized reward  $J^{(i)}(t_0^{(i)}, \dots)$  with respect to the policy parameters  $(\theta, \phi)$ :

$$\nabla_{(\theta, \phi)} J^{(i)}(t_0^{(i)}, x_0^{(i)}, \mathbf{y}_0^{(i)}; \theta, \phi).$$

This gradient serves as an unbiased estimate related to the gradient of the conditional expected utility  $J(t_0^{(i)}, \dots)$ .

5. **Estimate Gradient of  $\tilde{J}$ :** Obtain an unbiased estimate for the gradient of the overall extended objective  $\tilde{J}$  by averaging the individual path gradients over the mini-batch:

$$\nabla \tilde{J}(\theta, \phi) \approx \nabla_{\text{batch}} = \frac{1}{M} \sum_{i=1}^M \nabla_{(\theta, \phi)} J^{(i)}(t_0^{(i)}, x_0^{(i)}, \mathbf{y}_0^{(i)}; \theta, \phi).$$

6. **Update Policy Parameters:** Update the parameters  $(\theta, \phi)$  using this averaged gradient estimate via stochastic gradient ascent:

$$(\theta, \phi)_{j+1} \leftarrow (\theta, \phi)_j + \alpha_j \nabla_{\text{batch}},$$

where  $\alpha_j$  is the learning rate.

By iterating these steps, the baseline PG-DPO algorithm gradually optimizes the policy  $(\pi_\theta, C_\phi)$  to maximize the extended value function  $\tilde{J}$ .

---

**Algorithm 1** Baseline Pontryagin-Guided Direct Policy Optimization (PG-DPO)
 

---

**Inputs:**

**Require:** Policy nets  $\pi_\theta, C_\phi$ ; learning-rate schedule  $\{\alpha_j\}_{j=0}^{J_{\max}-1}$ ; max iters  $J_{\max}$ , batch size  $M$ , time steps  $N$ ; initial-state distribution  $\eta$ ; utility  $U$ , discount  $\delta$ , terminal weight  $\kappa$ ; market params  $(\boldsymbol{\mu}, \boldsymbol{\sigma}, r, \boldsymbol{\mu}_Y, \boldsymbol{\sigma}_Y, \boldsymbol{\Omega})$

**Output:** optimised params  $(\theta_{\text{opt}}, \phi_{\text{opt}})$

```

1: Initialise  $\theta, \phi$ 
2: for  $j = 0$  to  $J_{\max} - 1$  do
3:   Draw mini-batch  $\{(t_0^{(i)}, x_0^{(i)}, \mathbf{y}_0^{(i)})\}_{i=1}^M \sim \eta$ 
4:    $\nabla_{\text{batch}} \leftarrow \mathbf{0}$ 
5:   for  $i = 1$  to  $M$  do
6:      $(X_0, \mathbf{Y}_0) \leftarrow (x_0^{(i)}, \mathbf{y}_0^{(i)})$ ,  $\Delta t \leftarrow (T - t_0^{(i)})/N$ 
7:     for  $k = 0$  to  $N - 1$  do
8:        $t_k \leftarrow t_0^{(i)} + k\Delta t$ 
9:        $\boldsymbol{\pi}_k \leftarrow \pi_\theta(t_k, X_k, \mathbf{Y}_k)$ 
10:       $C_k \leftarrow C_\phi(t_k, X_k, \mathbf{Y}_k)$ 
11:      Sample  $\Delta \mathbf{W}_k \sim \mathcal{N}(\mathbf{0}, \boldsymbol{\Omega}\Delta t)$ 
12:       $\mathbf{Y}_{k+1} = \mathbf{Y}_k + \boldsymbol{\mu}_Y(t_k, \mathbf{Y}_k)\Delta t + \boldsymbol{\sigma}_Y(t_k, \mathbf{Y}_k) \Delta \mathbf{W}_k^Y$ 
13:       $X_{k+1} = X_k + \left[ X_k(r(t_k, \mathbf{Y}_k) + \boldsymbol{\pi}_k^\top(\boldsymbol{\mu}(t_k, \mathbf{Y}_k) - r(t_k, \mathbf{Y}_k)\mathbf{1})) - C_k \right] \Delta t + X_k \boldsymbol{\pi}_k^\top \boldsymbol{\sigma}(t_k, \mathbf{Y}_k) \Delta \mathbf{W}_k^X$ 
14:    end for
15:     $J^{(i)} = \sum_{k=0}^{N-1} e^{-\delta t_k} U(C_k) \Delta t + \kappa e^{-\delta T} U(X_N)$ 
16:     $g^{(i)} \leftarrow \nabla_{(\theta, \phi)} J^{(i)}$ 
17:     $\nabla_{\text{batch}} \leftarrow \nabla_{\text{batch}} + g^{(i)}$ 
18:  end for
19:   $(\theta, \phi) \leftarrow (\theta, \phi) + \frac{\alpha_j}{M} \nabla_{\text{batch}}$ 
20: end for
21: return  $(\theta, \phi)$ 

```

---

**Role of Intermediate BPTT Values and the ‘‘Pontryagin-Guided’’ Nature.** It is important to understand the role of the intermediate values computed during BPTT in Step 4. As BPTT calculates the policy gradient  $\nabla_{(\theta, \phi)} J^{(i)}(\dots)$  via the chain rule, it inherently computes the partial derivatives of the realized reward  $J^{(i)}(\dots)$  with respect to the intermediate states along path  $i$ :

$$\lambda_k^{(i)} = \frac{\partial J^{(i)}(t_0^{(i)}, \dots)}{\partial X_k^{(i)}}, \quad \boldsymbol{\eta}_k^{(i)} = \frac{\partial J^{(i)}(t_0^{(i)}, \dots)}{\partial \mathbf{Y}_k^{(i)}}.$$

These sensitivities, computed mechanically by AD, are directly linked to the discrete adjoint Backward Stochastic Differential Equation (BSDE) structure required by Pontryagin’s Maximum Principle (PMP). To illustrate this crucial connection for the wealth component (denoting  $\lambda_k^{(i)}$  for  $\lambda_k^{X, (i)}$  for simplicity), consider the discrete Euler-Maruyama step for wealth under policy  $(\boldsymbol{\pi}_k^{(i)}, C_k^{(i)})$ :

$$X_{k+1}^{(i)} = X_k^{(i)} + \left[ X_k^{(i)} \left( r(t_k, \mathbf{Y}_k^{(i)}) + \boldsymbol{\pi}_k^{(i)\top} (\boldsymbol{\mu}(t_k, \mathbf{Y}_k^{(i)}) - r(t_k, \mathbf{Y}_k^{(i)})\mathbf{1}) \right) - C_k^{(i)} \right] \Delta t + X_k^{(i)} \boldsymbol{\pi}_k^{(i)\top} \boldsymbol{\sigma}(t_k, \mathbf{Y}_k^{(i)}) \Delta \mathbf{W}_k^{(i)}.$$

Applying the chain rule one step backward ( $\lambda_k^{(i)} = \lambda_{k+1}^{(i)} \frac{\partial X_{k+1}^{(i)}}{\partial X_k^{(i)}}$ ) and using a first-order expansion yields the following backward recurrence relation along the path ( $i$ ):

$$\lambda_k^{(i)} \approx \lambda_{k+1}^{(i)} + \lambda_{k+1}^{(i)} [r + \boldsymbol{\pi}_k^{(i)\top} (\boldsymbol{\mu} - r)] \Delta t + \lambda_{k+1}^{(i)} \boldsymbol{\pi}_k^{(i)\top} \boldsymbol{\sigma} \Delta \mathbf{W}_k^{(i)}.$$

This equation inherently possesses the structure of a discrete BSDE operating along the specific simulation path ( $i$ ). To formally connect this to the BSDE formulation in PMP, which involves

processes adapted to the filtration  $\{\mathcal{F}_{t_k}\}$  (representing available information at time  $t_k$ ), one defines the adapted costate  $\lambda_k = \mathbb{E}[\lambda_k^{(i)} | \mathcal{F}_{t_k}]$  and the predictable martingale component  $Z_k$  (related to the conditional expectation of  $\lambda_{k+1}^{(i)} \Delta W_k^{(i)}$ ). Taking the conditional expectation ( $\mathbb{E}[\cdot | \mathcal{F}_{t_k}]$ ) of the pathwise recurrence relation above, and carefully defining  $Z_k$  using a covariation-based approach, leads precisely to the standard discrete BSDE for the adapted process  $\lambda_k$ :

$$\lambda_k = \lambda_{k+1} + \underbrace{(\lambda_{k+1}[r + \pi_k(\mu - r)] + \pi_k \sigma Z_k)}_{\approx \partial_x \mathcal{H}(t_k, \dots) \text{ from PMP}} \Delta t - Z_k \Delta W_k. \quad (13)$$

Crucially, the drift term derived through this process corresponds exactly to the derivative of the discrete-time Hamiltonian ( $\partial_x \mathcal{H}$ ) from PMP with respect to the state variable  $x$ . A similar structure holds for the costate vector  $\boldsymbol{\eta}_k$  associated with the state variables  $\mathbf{Y}_k$ .

Therefore, the values  $\lambda_k^{(i)}$  and  $\boldsymbol{\eta}_k^{(i)}$  computed by BPTT are indeed pathwise numerical counterparts related to the Pontryagin costates, satisfying the relevant discrete BSDE structure. Crucially, in the *baseline* PG-DPO algorithm, these costate estimates themselves (and their potential derivatives w.r.t. states) are **not directly used** in the parameter update rule (Step 6), which only requires the final gradient  $\nabla_{(\theta, \phi)} J^{(i)}(\dots)$ .

Nevertheless, the fact that BPTT provides access to these theoretically grounded estimates is fundamental. Firstly, they are essential inputs for the **Two-Stage PG-DPO** variant discussed in the next subsection (§3.2). The baseline algorithm thus lays the groundwork by generating these estimates. Secondly, this deep connection explains why the algorithm is termed **Pontryagin-Guided**. Even though the baseline update only uses  $\nabla_{(\theta, \phi)} J^{(i)}(\dots)$ , the calculation of this gradient via BPTT structurally mirrors the backward propagation of sensitivities inherent in PMP’s adjoint equations (BSDEs), using the costate estimates  $\lambda_k^{(i)}, \boldsymbol{\eta}_k^{(i)}$  implicitly within the chain rule (cf. Huh, 2024). Consequently, the optimization process, driven by these BPTT-computed gradients, is implicitly guided by the optimality conditions derived from Pontryagin’s principle, aiming to maximize the expected objective  $\tilde{J}$ .

### 3.2 Two-Stage PG-DPO Algorithm

While the baseline PG-DPO algorithm described in Section 3.1 effectively optimizes the extended objective  $\tilde{J}$  by training the policy networks  $(\boldsymbol{\pi}_\theta, C_\phi)$  end-to-end, it can sometimes require a significant number of iterations for the networks to fully converge. The Two-Stage PG-DPO variant offers a potentially more computationally efficient alternative by exploiting an empirical observation: the costate estimates  $(\lambda_k^{(i)}, \boldsymbol{\eta}_k^{(i)})$  and their relevant derivatives with respect to states, like  $\partial_x \lambda_k^{(i)}, \partial_{\mathbf{Y}} \lambda_k^{(i)}$ , which are generated during BPTT, often stabilize and become reasonably accurate much faster than the full policy networks achieve optimality.

This Two-Stage approach leverages these rapidly stabilizing costate estimates to construct near-optimal controls directly from the PMP first-order conditions, bypassing the need for fully converged policy networks for deployment. The procedure consists of two distinct stages, described below using a single level of enumeration:

#### 1. Stage 1: Warm-Up Phase for Costate Estimation

First, we execute the **Baseline PG-DPO process**, as detailed in Section 3.1 (which optimizes  $\tilde{J}$ ), for a predetermined, relatively small number of iterations,  $K_0$ . The primary objective of this stage is **not** to obtain fully optimized networks  $(\boldsymbol{\pi}_\theta, C_\phi)$ , but rather to run the BPTT process sufficiently long for the underlying mechanism generating the **costate estimates**  $(\lambda_k^{(i)} = \partial J^{(i)}(\dots) / \partial X_k^{(i)}, \boldsymbol{\eta}_k^{(i)} = \partial J^{(i)}(\dots) / \partial \mathbf{Y}_k^{(i)})$  and their relevant state-derivatives (e.g.,  $\partial_x \lambda_k^{(i)}, \partial_{\mathbf{Y}} \lambda_k^{(i)}$ ) to stabilize. We let  $(\theta^*, \phi^*)$  denote the policy parameters obtained at the end of this warm-up phase.

---

**Algorithm 2** Two-Stage PG-DPO: Warm-up Training & Deployment
 

---

**Stage 1: Warm-up Training**
**Require:** Inputs of Algorithm 1; warm-up iterations  $K_0$ 
**Ensure:** Stabilised parameters  $(\theta^*, \phi^*)$ 

- 1: Run Algorithm 1 for  $K_0$  iterations to obtain  $(\theta^*, \phi^*)$

**Stage 2: Deployment at state  $(t, X, \mathbf{Y})$** 
**Require:** State  $(t, X, \mathbf{Y})$ ; parameters  $(\theta^*, \phi^*)$ ; Monte-Carlo rollouts  $M_{\text{MC}}$ , steps  $N'$ 
**Ensure:** Near-optimal controls  $(\pi^{\text{PMP}}, C^{\text{PMP}})$ 

- 2: Initialise  $\mathcal{L}, \mathcal{L}_x, \mathcal{L}_Y \leftarrow \emptyset$
  - 3: **for**  $j = 1$  **to**  $M_{\text{MC}}$  **do**
  - 4:   Simulate path with  $(\pi_{\theta^*}, C_{\phi^*})$  using  $N'$  steps
  - 5:   Compute realized reward for path  $j$ :
  - 6:   
$$J^{(j)} \leftarrow \sum_{n=0}^{N'-1} e^{-\delta t_n} U(C_{t_n}^{(j)}) \Delta t' + \kappa e^{-\delta T} U(X_T^{(j)})$$
  - 7:   Evaluate  $\lambda_t^{(j)}, \partial_x \lambda_t^{(j)}, \partial_Y \lambda_t^{(j)}$  and append
  - 8: **end for**
  - 9: Compute  $\hat{\lambda}_t, \widehat{\partial_x \lambda}_t, \widehat{\partial_Y \lambda}_t$  ▷ E.g., by averaging estimates from loop
  - 10:  $C^{\text{PMP}} \leftarrow (U')^{-1}(e^{\delta t} \hat{\lambda}_t)$  ▷ Using PMP FOC Eq. (8)
  - 11: Compute  $\pi^{\text{PMP}}$  via PMP FOC Eq. (15) ▷ Using estimated costates/derivatives
  - 12: **return**  $(\pi^{\text{PMP}}, C^{\text{PMP}})$
- 

**2. Stage 2: Analytic Control Deployment**

After completing the  $K_0$  warm-up iterations, the trained policy networks  $(\pi_{\theta^*}, C_{\phi^*})$  are typically **not directly used** for generating controls during deployment. Instead, to determine the control actions for any given state  $(t_k, X_k, \mathbf{Y}_k)$  encountered during deployment, we employ a Monte Carlo-like averaging procedure to obtain reliable costate estimates needed for the PMP formulas:

First, to obtain the **stabilized costate estimates** corresponding to the state  $(t_k, X_k, \mathbf{Y}_k)$ , we perform the following averaging: Simulate multiple ( $M_{\text{MC}}$ ) forward paths starting from  $(t_k, X_k, \mathbf{Y}_k)$  (or states very close to it) up to the horizon  $T$ , using the *fixed* policy parameters  $(\theta^*, \phi^*)$  obtained from Stage 1. For each simulated path  $j = 1, \dots, M_{\text{MC}}$ , calculate its realized reward  $J^{(j)}(t_k, X_k, \mathbf{Y}_k; \theta^*, \phi^*)$  and apply BPTT to obtain the costate estimates  $\lambda_k^{(j)}, \partial_x \lambda_k^{(j)}, \partial_Y \lambda_k^{(j)}$  specifically at the starting node  $k$  for that path  $j$ . The final “stabilized” estimates are then computed by averaging these values across the  $M_{\text{MC}}$  paths:

$$\lambda_k \approx \frac{1}{M_{\text{MC}}} \sum_{j=1}^{M_{\text{MC}}} \lambda_k^{(j)}, \quad \partial_x \lambda_k \approx \frac{1}{M_{\text{MC}}} \sum_{j=1}^{M_{\text{MC}}} \partial_x \lambda_k^{(j)}, \quad \partial_Y \lambda_k \approx \frac{1}{M_{\text{MC}}} \sum_{j=1}^{M_{\text{MC}}} \partial_Y \lambda_k^{(j)}$$

This averaging acts as a Monte Carlo estimation step, significantly reducing the variance inherent in the single-path BPTT estimates derived during Stage 1 and providing more robust inputs for the PMP formulas.

Next, we plug these **averaged costate estimates**  $(\lambda_k, \partial_x \lambda_k, \partial_Y \lambda_k)$  directly into the analytical formulas derived from the Pontryagin Maximum Principle’s first-order conditions (Section 2.2). The optimal consumption is calculated as:

$$C_k^{\text{PMP}} = (U')^{-1}(e^{\delta t_k} \lambda_k).$$

The optimal investment portfolio is calculated as:

$$\boldsymbol{\pi}_k^{\text{PMP}} = -\frac{1}{X_k \partial_x \lambda_k} \Sigma^{-1}(t_k, \mathbf{Y}_k) \left\{ \lambda_k [\boldsymbol{\mu}(t_k, \mathbf{Y}_k) - r(t_k, \mathbf{Y}_k) \mathbf{1}] \right. \quad (14)$$

$$\left. + \boldsymbol{\sigma}(t_k, \mathbf{Y}_k)^\top (\partial_{\mathbf{Y}} \lambda_k) \boldsymbol{\sigma}_Y(t_k, \mathbf{Y}_k) \boldsymbol{\rho}^\top \Psi^{-1} \right\}. \quad (15)$$

Finally, these analytically computed values  $(C_k^{\text{PMP}}, \boldsymbol{\pi}_k^{\text{PMP}})$ , based on the averaged costate estimates, are used as the control actions for the state  $(t_k, X_k, \mathbf{Y}_k)$  during deployment.

In summary, the Two-Stage PG-DPO approach performs a short warm-up training (Stage 1) using the baseline PG-DPO process to obtain a policy  $(\theta^*, \phi^*)$  whose BPTT generates reasonably stable costate estimates. It then leverages these estimates in Stage 2, refining them through Monte Carlo averaging at the point of deployment and plugging them into the known analytical structure of the optimal control derived from PMP. This strategy can significantly reduce the overall computational burden while yielding high-quality, near-optimal controls. The Monte Carlo averaging step in Stage 2 is crucial for obtaining reliable inputs for the PMP formulas from the potentially noisy single-path estimates.

### 3.3 Rationale for the Two-Stage Approach

#### 3.3.1 The Parabolic Nature of Financial Models and PDE Regularity

In continuous-time financial models, where the dynamics of investor wealth  $X_t$  and exogenous state variables  $\mathbf{Y}_t$  are modeled by stochastic differential equations (SDEs), the Value Function  $V(t, X_t, \mathbf{Y}_t)$  for a dynamic optimization problem typically solves a Hamilton–Jacobi–Bellman (HJB) partial differential equation (PDE) (e.g., Fleming & Soner, 2006; Yong & Zhou, 2012). This HJB equation exhibits a **parabolic** form. The specific nature of its parabolicity is primarily determined by the **diffusion coefficients** of the underlying SDEs, namely  $\boldsymbol{\sigma}$  (related to assets) and  $\boldsymbol{\sigma}_Y$  (related to state variables). While the drift coefficients  $(\boldsymbol{\mu}, \boldsymbol{\mu}_Y)$  influence the first-order terms in the HJB and are crucial for the solution’s properties, they do not dictate the type of parabolicity, which is mainly governed by the second-order terms (diffusion).

The behavior of the diffusion matrix  $a(t, x, \mathbf{y})$  (the matrix multiplying second-order derivatives in the HJB equation) allows for classifying parabolic PDEs into three main classes (see, e.g., Evans, 2022). This classification significantly impacts the **regularity** (smoothness) of the Value Function  $V$  and its associated Costates (the first-order derivatives  $\nabla V$ ) (cf. Evans, 2022, Ch. 6-7). Costates represent the sensitivity of the Value Function, and Pontryagin’s Maximum Principle links optimal Costates to the optimal policy. The core idea of Two-Stage PG-DPO involves estimating Costates and their derivatives via BPTT and using these estimates in the PMP formulas. Therefore, the regularity of the Costates—tied to the model’s parabolicity class—directly affects the difficulty of Costate estimation and the effectiveness of the Two-Stage method.

The table 1 summarizes these classes, their properties, links to SDE coefficients, and relevant examples within the dynamic portfolio optimization context.

Models falling into classes (U) and (H) are expected to possess sufficiently regular Costates, providing a favorable setting for the estimation required by the Two-Stage PG-DPO method. The numerical experiments in this paper are conducted using models belonging to classes (U) or (H), where the Two-Stage PG-DPO effectively leverages the expected regularity of the Costates. The method is particularly effective as it generally avoids visiting degenerate boundaries during practical implementation.

Table 1: Classification of Parabolic HJB PDEs in Financial Models

Class	Diffusion Matrix $a(t, x, \mathbf{y})$ Property	SDE Coefficient Requirements and Dynamic Portfolio Examples
<b>(U) Uniformly Elliptic</b>	Uniformly positive definite across the state space	The diffusion coefficients $\sigma$ (for wealth $X_t$ ) and $\sigma_Y$ (for state $\mathbf{Y}_t$ ) are such that the resulting diffusion matrix in the HJB is non-zero and bounded below by a positive constant everywhere ( $\sigma\Psi\sigma^\top$ and $\sigma_Y\Phi\sigma_Y^\top$ uniformly positive definite). Drift coefficients $(\mu, \mu_Y)$ are also sufficiently regular (e.g., Lipschitz). <b>Examples:</b> Merton's portfolio problem with constant coefficients ( $\mu, \sigma > 0, r$ are constants); models with state-dependent volatility that remains strictly positive; the multi-asset OU model in Section 2.3.1 (if asset volatilities $\sigma_i > 0$ , factor volatility $\sigma_Y > 0$ , and $\Psi$ is positive definite).
( $\implies$ Value Function / Costate very smooth)		
<b>(H) Hypo-elliptic / Uniform on Compacts</b>	May degenerate at some points, but regularity is achieved via system structure (e.g., drift-diffusion coupling via Hörmander's condition) or holds within a compact domain of interest. Degeneracy occurs away from boundaries.	Diffusion coefficients ( $\sigma$ or $\sigma_Y$ ) can become zero at certain points within the domain. However, interaction with non-zero drift terms or other diffusion terms maintains regularity.  <b>Examples:</b> The multi-asset multi-factor model in Section 2.3.2 (if some factor volatilities in $\sigma_Y$ can be zero at certain states but the overall system structure, possibly involving $\kappa_Y$ , ensures hypo-ellipticity); a Vasicek interest rate model affecting asset returns $\mu$ but not $\sigma$ .
( $\implies$ Value Function / Costate smooth in relevant regions)		
<b>(D) Degenerate at the Boundary</b>	Degenerates ( $\rightarrow 0$ ) as the state approaches a boundary.	The diffusion coefficients $\sigma$ or $\sigma_Y$ (or the combined diffusion matrix) approach zero as a state variable (e.g., wealth, volatility, interest rate) approaches a boundary (typically 0). <b>Examples:</b> CIR (Cox-Ingersoll-Ross) interest rate/volatility model (diffusion term like $\sigma_Y\sqrt{Y_t}$ ); Heston stochastic volatility model (asset diffusion term like $\sigma\sqrt{\nu_t}$ ).
( $\implies$ Value Function / Costate regularity may break down near the boundary)		

### 3.3.2 Mathematical Foundation: Derivative Stability via PDE Comparison

A key theoretical insight, particularly demonstrable in well-structured (e.g., affine) models, comes from analyzing the stability of value function derivatives under policy perturbations using regularity theory for parabolic partial differential equations (e.g., Evans, 2022; Krylov, 2024). This perspective illustrates how closeness of policies (in a specific sense) can imply closeness of derivatives, providing a foundation for why the Two-Stage approach might be effective.

First, let us recall the PDE associated with a given policy. For an admissible and sufficiently smooth policy  $(\pi(t, z), c(t, z))$ , where  $z = (x, y)$  represents the state, the corresponding value function  $V(t, z)$  (representing the expected utility achieved under this \*specific\* policy from state  $z$  at time  $t$ ) satisfies the linear parabolic PDE:

$$-\frac{\partial V}{\partial t} = \mathcal{L}_{\pi, c}[V](t, z) + f_{\pi, c}(t, z), \quad \text{subject to } V(T, z) = g(z). \quad (16)$$

Here,  $g(z) = \kappa e^{-\delta T} U(x)$  is the terminal utility,  $f_{\pi, c}(t, z) = e^{-\delta t} U(c(t, z))$  is the instantaneous utility source term under policy  $c$ , and  $\mathcal{L}_{\pi, c}$  is the second-order linear differential generator associated with the state dynamics under policy  $(\pi, c)$ :

$$\begin{aligned} \mathcal{L}_{\pi, c}[V] = & V_x \left[ x \left( (1 - \pi^\top \mathbf{1}) r(t, y) + \pi^\top \mu(t, y) \right) - c(t, z) \right] + V_y^\top \mu_Y(t, y) \\ & + \frac{1}{2} V_{xx} x^2 \pi^\top \sigma(t, y) \Psi \sigma(t, y)^\top \pi \\ & + V_{xy}^\top x \pi^\top \sigma(t, y) \rho \sigma_Y(t, y)^\top \\ & + \frac{1}{2} \text{Tr} \left( V_{yy} \sigma_Y(t, y) \Phi \sigma_Y(t, y)^\top \right) - \delta V \end{aligned} \quad (17)$$

(We incorporate the time discount term  $-\delta V$  into the operator  $\mathcal{L}_{\pi, c}$  for convenience). Let  $V^*(t, z)$  denote the true optimal value function of the control problem defined in Section 2.1, achieved by the optimal policy  $(\pi^*(t, z), c^*(t, z))$ . Assuming sufficient regularity,  $V^*$  satisfies the non-linear Hamilton-Jacobi-Bellman (HJB) equation (Fleming & Soner, 2006), which implies it also satisfies the linear PDE (16) when the optimal policy  $(\pi^*, c^*)$  is used:

$$-\frac{\partial V^*}{\partial t} = \mathcal{L}_{\pi^*, c^*}[V^*](t, z) + f_{\pi^*, c^*}(t, z), \quad \text{subject to } V^*(T, z) = g(z). \quad (18)$$

To formalize the notion of policy closeness relevant to the PDE coefficients, we introduce the following definition. Let  $\Sigma_{\text{asset}}(t, y) = \sigma(t, y) \Psi \sigma(t, y)^\top$  and  $\Sigma_{\text{asset-state}}(t, y) = \sigma(t, y) \rho \sigma_Y(t, y)^\top$ .

**Definition 1** (Coefficient-relevant  $\epsilon$ -closeness). *Let the spatial domain be*

$$\Omega \subseteq (0, \infty) \times \mathbb{R}^k, \quad z = (x, \mathbf{y}) \in \Omega,$$

*i.e.  $x$  is wealth and  $\mathbf{y} \in \mathbb{R}^k$  is the  $k$ -dimensional state vector. (In practice  $\Omega$  can be either the full space or a bounded truncated box that contains the region the process visits with high probability.)*

*Fix exponents  $p > d + 2$  and  $q \geq 2$ , where  $d = \dim \Omega = k + 1$ . For any measurable function  $h(t, z)$  set*

$$\|h\|_{L^{q,p}} := \left( \int_0^T \left[ \int_\Omega |h(t, z)|^p dz \right]^{q/p} dt \right)^{1/q}, \quad L^{q,p} = L^q(0, T; L^p(\Omega)).$$

*Let  $(\pi^*, c^*)$  be the optimal policy and  $(\pi, c)$  any admissible policy. We say  $(\pi, c)$  is  $(\epsilon, p, q)$ -*

close to  $(\pi^*, c^*)$  on  $Q_T = (0, T) \times \Omega$  if

$$\begin{aligned} \|c - c^*\|_{L^{q,p}} &\leq \epsilon, \\ \|\pi^\top \mathbf{1} - \pi^{*\top} \mathbf{1}\|_{L^{q,p}} &\leq \epsilon, \\ \|\pi^\top \boldsymbol{\mu} - \pi^{*\top} \boldsymbol{\mu}\|_{L^{q,p}} &\leq \epsilon, \\ \|\pi^\top \Sigma_{asset} \pi - \pi^{*\top} \Sigma_{asset} \pi^*\|_{L^{q,p}} &\leq \epsilon, \\ \|\pi^\top \Sigma_{asset-state} - \pi^{*\top} \Sigma_{asset-state}\|_{L^{q,p}} &\leq \epsilon. \end{aligned}$$

**Proposition 3.1** (Derivative closeness under coefficient  $\epsilon$ -closeness). *Let  $V^*$  be the optimal value function corresponding to the optimal policy  $(\pi^*, c^*)$  (cf. (18)) and let  $V$  be the value function generated by another admissible policy  $(\pi, c)$  (cf. (16)). Set*

$$D := V^* - V, \quad Q_T := (0, T) \times \Omega.$$

Assume

(A1) **Uniform parabolicity.** *The operator  $\mathcal{L}_{\pi^*, c^*}$  is uniformly parabolic on  $Q_T$ .*

(A2) **Baseline regularity.** *There exist exponents  $p > d+2$  and  $q \geq 2$  (with  $d = \dim \Omega = k+1$ ) such that the value functions lie in the Sobolev space (e.g., Adams & Fournier, 2003; Evans, 2022)*

$$V^*, V \in L^q(0, T; W^{2,p}(\Omega)).$$

(A3) **Coefficient  $\epsilon$ -closeness.** *The candidate policy  $(\pi, c)$  is  $(\epsilon, p, q)$ -close to  $(\pi^*, c^*)$  in the sense of Definition 1.*

Then  $D$  satisfies the linear PDE

$$-\partial_t D = \mathcal{L}_{\pi^*, c^*}[D] + S', \quad \text{where } S' = (\mathcal{L}_{\pi^*, c^*} - \mathcal{L}_{\pi, c})[V] + (f_{\pi^*, c^*} - f_{\pi, c}).$$

Moreover, the source term is small in the weighted norm:

$$\|S'\|_{L^{q,p}} \leq C_0 \epsilon,$$

and by standard  $L^p$  / Schauder estimates for uniformly parabolic equations (see, e.g., Evans, 2022, Ch. 7),

$$\|D\|_{L^q(0, T; W^{2,p}(\Omega))} \leq C \|S'\|_{L^{q,p}} \leq C \epsilon,$$

for a constant  $C$  independent of  $\epsilon$ .

Consequently, the value-function gap and all first- and second-order spatial derivatives satisfy

$$\|V^* - V\|_{L^{q,p}} + \|\nabla V^* - \nabla V\|_{L^{q,p}} + \|D^2 V^* - D^2 V\|_{L^{q,p}} \leq C \epsilon.$$

Hence the costates  $(\nabla V)$  produced under  $(\pi, c)$  are  $O(\epsilon)$ -close to the optimal costates on the entire space-time domain.

### Remark on assumptions, PG–DPO rationale, and scope of the result.

Proposition 3.1 makes precise the intuition for the **uniformly-parabolic class** (“U class”): if two policies yield *close PDE-coefficients* in the weak sense of Definition 1 (only a global<sup>1</sup>  $L^{q,p}$ -distance), then their value functions—and hence their gradients (costates)—differ by at most  $O(\epsilon)$ . Assumptions (A1)–(A2) are the classical entry ticket for  $L^p$  / Schauder regularity (Evans, 2022) and are easily verified for *affine* models or for models that become uniformly elliptic

<sup>1</sup>A still weaker *occupation-weighted* norm is discussed below.

after adding a *small floor* to each diffusion coefficient (e.g. replace  $\sigma(t, z)$  by  $\sqrt{\sigma(t, z)^2 + \varepsilon^2}$  with  $\varepsilon \sim 10^{-4}$ ). Such a floor leaves the economics virtually unchanged while preventing the diffusion matrix from collapsing to zero, which is exactly what uniform parabolicity requires. The genuinely new ingredient is (A3), the  $\epsilon$ -coefficient closeness that Stage 1 of PG-DPO is designed to enforce.

Stage 1 produces a sub-optimal policy  $(\pi, c)$  whose coefficient error is  $\epsilon$ . Via Proposition 3.1 this translates into an  $O(\epsilon)$  error for the costate  $\lambda \approx \nabla V$ , so the BPTT outputs obtained during the short warm-up are already  $O(\epsilon)$ -accurate surrogates of the true optimal costates. Stage 2 simply substitutes these estimates into the PMP first-order conditions (Pontryagin, 2014; Yong & Zhou, 2012), thereby constructing a near-optimal control without having to train the policy network to full convergence.

*Global vs. – local norms.* – The result is stated with a *global*  $\|\cdot\|_{L^{q,p}}$  norm for transparency. If desired, one may replace it by the occupation-weighted norm

$$\|h\|_{L^{q,p}(\mu_{(\pi,c)})} := \left( \int_0^T \left[ \int_{\Omega} |h(t, z)|^p \mu_{(\pi,c)}(t, z) dz \right]^{q/p} dt \right)^{1/q},$$

where  $\mu_{(\pi,c)}$  is the state-density under the candidate policy. Because the proof relies on local PDE estimates, the same  $O(\epsilon)$  bound holds—now only on the subset of the state space that the process actually visits with non-negligible probability. This is valuable for models whose coefficients degenerate in remote regions.

*Beyond the U class.* – For **hypo-elliptic** (H class) (cf. Hörmander, 1967) or **boundary-degenerate** (D class) models (e.g., Oleinik, 2012), the full global  $L^p$  theory is subtler, yet the algorithmic logic of Two-Stage PG-DPO is unaffected:

- the PMP equations and BPTT apply to any differentiable dynamics;
- costates typically stabilise faster than the full optimal control;
- a brief warm-up that makes the coefficient error small *where it matters* is enough to obtain high-quality costate estimates.

Even when the rigorous guarantee of Proposition 3.1 is unavailable, this costate-first, PMP-second recipe remains an effective practical strategy—an observation confirmed empirically in the numerical section (Section 4) and worth exploring further for genuinely non-affine or degenerate models.

### 3.3.3 Qualitative Rationale and Broader Applicability

While the formal analysis in Proposition 3.1 provides rigorous support under specific regularity conditions (like uniform parabolicity, often associated with affine models), the core ideas underpinning the Two-Stage PG-DPO approach possess a broader qualitative appeal that suggests applicability beyond these settings.

Crucially, neither the Pontryagin Maximum Principle (PMP) itself (Pontryagin, 2014; Yong & Zhou, 2012) nor the mechanics of backpropagation-through-time (BPTT) (e.g., Goodfellow, 2016) are inherently restricted to affine or uniformly parabolic systems. PMP provides necessary optimality conditions for general nonlinear dynamics, provided the required functions are differentiable. Similarly, BPTT serves as a general algorithm for computing gradient estimates through complex computational graphs derived from simulations, regardless of the underlying model’s linearity.

Furthermore, there is a compelling economic and mathematical intuition that the PMP costates ( $\lambda \approx \nabla V$ , representing marginal values) might exhibit properties that make them more amenable to estimation than the potentially complex optimal policy  $\pi^*$  itself, especially

in high-dimensional problems. For instance, the costate functions might be representable by smoother or lower-complexity functions compared to  $\pi^*$ . Alternatively, the process of learning or estimating these costate-related functions via BPTT with neural networks might converge more rapidly or stably than directly learning the intricate mapping defined by the optimal policy.

The Two-Stage PG-DPO strategy is designed precisely to leverage this potential advantage. It effectively decouples the optimization challenge into two parts: (i) tackling the potentially more tractable task of estimating costates (and their relevant derivatives) using BPTT during a warm-up phase; (ii) employing the robust analytical structure of the PMP first-order conditions to translate these estimates into effective control actions during deployment.

Therefore, even in scenarios where the rigorous derivative closeness guarantees of Proposition 3.1 are harder to establish formally (e.g., for non-affine models, or systems falling into the hypo-elliptic or degenerate parabolic classes), this underlying qualitative rationale remains persuasive. The potential for BPTT-derived costate estimates to stabilize relatively quickly and capture essential optimality information offers a strong motivation for exploring the Two-Stage PG-DPO approach in these more complex settings.

This rationale, significantly reinforced by the numerical success demonstrated in the affine benchmark case (Section 4), positions PG-DPO (particularly the superior Two-Stage variant) as a promising and potentially powerful tool for tackling challenging high-dimensional, possibly non-affine, continuous-time control problems prevalent in finance and other domains. Naturally, its practical effectiveness in such extended settings must be carefully evaluated empirically on a case-by-case basis, highlighting an important direction for future research.

## 4 Numerical Experiments

In this section, we conduct numerical experiments to evaluate the performance and scalability of the proposed PG-DPO framework (both Baseline and Two-Stage variants). We focus on the multi-asset, multi-factor Ornstein-Uhlenbeck (OU) portfolio optimization problem introduced in Section 2.3.2. The objective is to maximize the expected utility of terminal wealth,  $J = \mathbb{E}[U(X_T)]$ , using a CRRA utility function with risk aversion  $\gamma = 2.0$ . This specific affine model setting allows for comparison against a semi-analytical benchmark solution derived from the HJB equation (details in Appendix B.2). We compare the policies generated by Baseline PG-DPO and Two-Stage PG-DPO against this benchmark using the Root Mean Squared Error (RMSE) metric across various dimensions, scaling up to  $n=50$  assets and  $k=10$  state factors. For complete details on the specific parameter values, PG-DPO implementation (network architecture, training setup), benchmark computation, and evaluation procedures, please refer to Appendix C. The subsequent subsections present and analyze the results.

### 4.1 Convergence Speed and Accuracy Analysis

This section quantitatively compares the convergence speed and final accuracy of the proposed PG-DPO methodologies across various dimensional settings. Figure 1 displays the average Root Mean Squared Error (RMSE), averaged across  $k = 10$  evaluation slices, between the learned policies (either  $\pi_\theta$  for Baseline PG-DPO or  $\pi^{\text{PMP}}$  for Two-Stage PG-DPO) and the benchmark optimal policy ( $\pi^*$ ). The RMSE is plotted as a function of training epochs on a logarithmic scale for configurations with  $k = 10$  state variables and varying numbers of assets ( $n = 1, 10, 50$ ).

The RMSE for the Two-Stage PG-DPO (orange line in Figure 1) represents the error of the total portfolio policy  $\pi^{\text{PMP}}$  constructed by substituting the BPTT-derived costate estimates into the PMP first-order condition (Eq. (10)). A key advantage is that the Two-Stage approach explicitly combines the analytically distinct *myopic* and *hedging* components. As established theoretically and confirmed numerically (see Section 4.2), the error of the myopic component

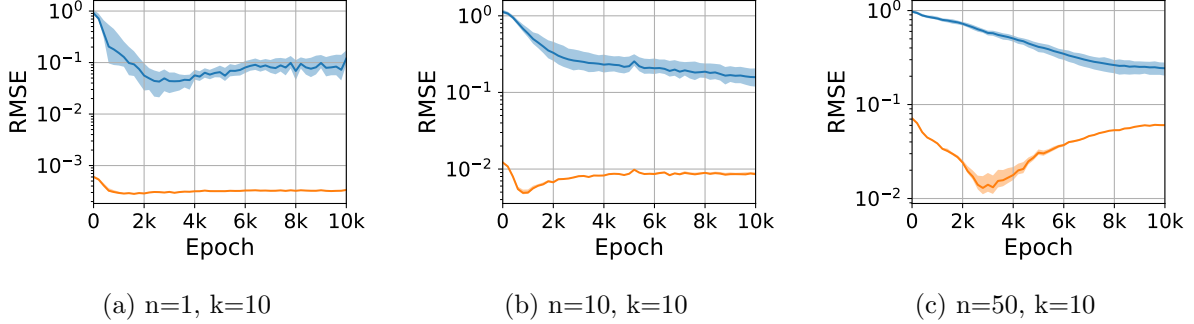


Figure 1: Average policy RMSE comparison between Baseline PG-DPO (blue) and Two-Stage PG-DPO (orange) relative to the benchmark solution across different dimensions ( $k=10$  fixed). Values averaged over  $k$  evaluation slices. Note the logarithmic scale on the y-axis.

is typically negligible (e.g., on the order of  $10^{-7}$ ). Therefore, the total RMSE for the Two-Stage policy is **almost entirely attributable to the error in estimating the hedging component**. This highlights the proficiency of the Two-Stage method in accurately capturing hedging demands using BPTT-derived costate derivatives ( $\partial_{\mathbf{Y}} \lambda_t^*$ ).

The key finding from Figure 1 and summarized in Table 2 is the consistent and significant outperformance of the Two-Stage PG-DPO method. Table 2 shows that **Two-Stage PG-DPO achieves minimum RMSE values dramatically lower than the Baseline method across all dimensions**—approximately 150 times lower for  $n = 1$ , 30 times lower for  $n = 10$ , and nearly 10 times lower for  $n = 50$ . Furthermore, **2-PG-DPO typically reaches its minimum error much earlier** in the training process (e.g., at epoch 1,500 vs. 2,600 for  $n = 1, k = 10$ , and epoch 800 vs. 10,000 for  $n = 10, k = 10$ ). Notably, while the convergence time for Baseline PG-DPO appears to increase substantially with the problem dimension ( $n$ ), the time required for 2-PG-DPO to reach its minimum error seems relatively less sensitive to the number of assets. Even in the high-dimensional  $n = 50, k = 10$  setting, 2-PG-DPO finds a near-optimal solution with an RMSE of  $1.32 \times 10^{-2}$  around epoch 3200, whereas the Baseline method’s minimum RMSE of  $1.26 \times 10^{-1}$  is reached only at the end of a much longer training period (epoch 100,000).

This clearly demonstrates the superiority of the Two-Stage approach and strongly supports the rationale discussed in Section 3.3: leveraging the PMP structure via BPTT-estimated costates is more efficient and accurate than end-to-end policy approximation, especially as dimensionality increases. The subsequent section presents a detailed visual analysis for the most

Table 2: Summary of Minimum Achieved Policy RMSE and Convergence Epochs

Dimension ( $n$ assets, $k$ factors)	Method	Min. Policy RMSE (vs. Benchmark)	Epochs at Min.
$n=1, k=10$	Baseline PG-DPO	$4.27 \times 10^{-2}$	2,600
	2-PG-DPO	$2.80 \times 10^{-4}$	1,500
$n=10, k=10$	Baseline PG-DPO	$1.58 \times 10^{-1}$	10,000
	2-PG-DPO	$4.89 \times 10^{-3}$	800
$n=50, k=10$	Baseline PG-DPO	$1.26 \times 10^{-1}$	100,000
	2-PG-DPO	$1.32 \times 10^{-2}$	3,200

Note: Minimum Policy RMSE values are averaged across the  $k = 10$  evaluation slices. Epochs indicate the recorded iteration number when the minimum average RMSE was observed; evaluations and logging were performed every 200 iterations.

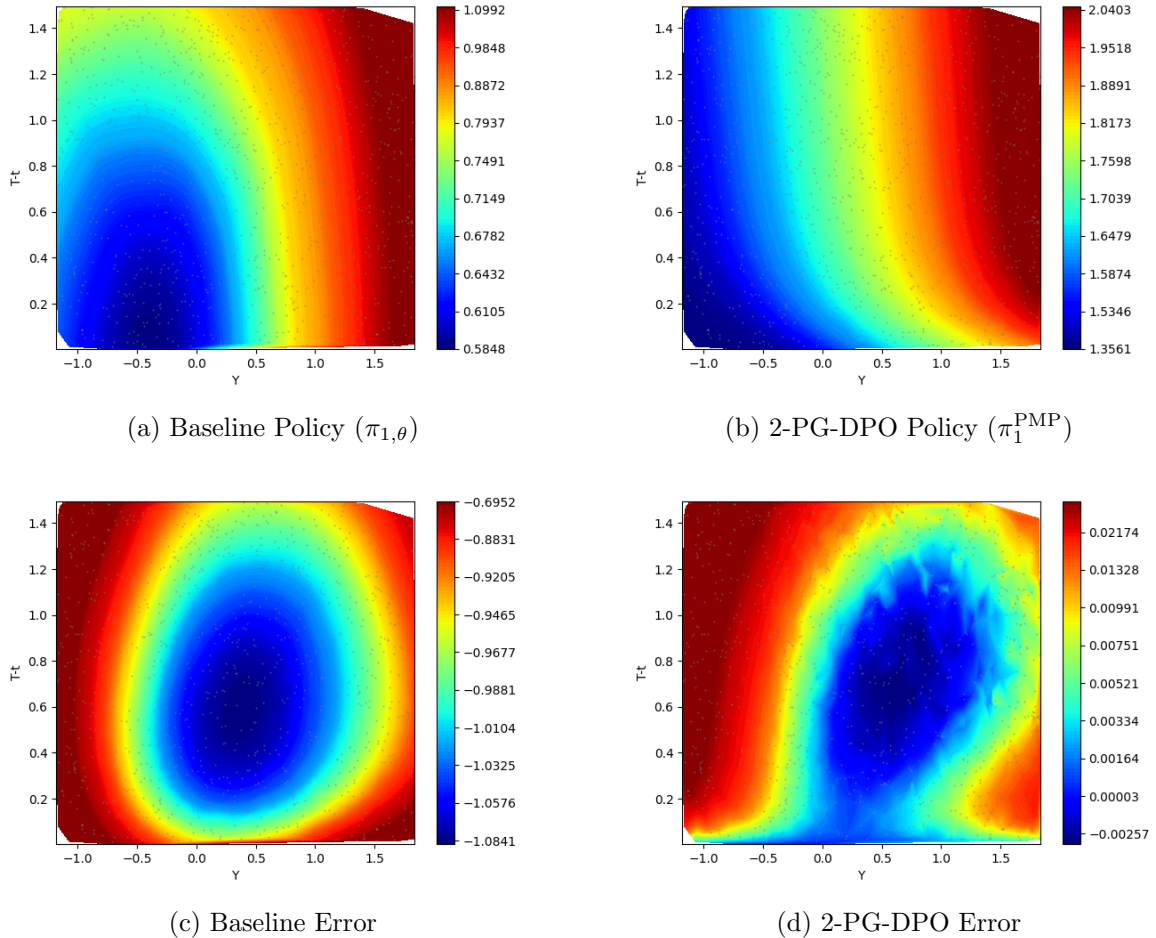


Figure 2: Comparison of total policies and errors for the first asset ( $i = 1$ ) in the  $n=50, k=10$  case on epoch 3,200 (plotted against  $Y_1$ ). Top row compares policies, bottom row compares errors (using Symlog scale). Note the significantly different color bar ranges are used for each plot to best visualize its content, reflecting the dramatic difference in policy/error magnitudes.

challenging high-dimensional case ( $n = 50, k = 10$ ) to further illustrate the performance difference. Hereafter, we often abbreviate Two-Stage PG-DPO as 2-PG-DPO.

## 4.2 High-Dimensional Performance Analysis ( $n=50, k=10$ )

We now visually examine the performance in the most challenging setting:  $n = 50$  assets and  $k = 10$  state variables. This scenario tests scalability where traditional DP methods are intractable. As shown quantitatively in Table 2 and Figure 1c, the 2-PG-DPO method achieves a minimum RMSE ( $1.32 \times 10^{-2}$  at epoch 3,200) significantly better than the Baseline approach ( $1.26 \times 10^{-1}$  at epoch 100,000).

The visualizations in Figures 2 and 3 focus on the policy for the first asset ( $i = 1$ ) versus time-to-maturity ( $T - t$ ) and the first state variable ( $Y_1$ ), holding other state variables constant at their long-term means. The results shown correspond to the state on epoch 3,200, near where the 2-PG-DPO method achieved its minimum observed RMSE.

The challenges of high dimensionality become starkly evident for the Baseline PG-DPO method in Figure 2. While the learned policy (a) shows some structure, the corresponding error (c) is extremely large, visually confirming the poor quantitative performance reported in Table 2. This indicates severe inaccuracies in the policy learned by the Baseline method when

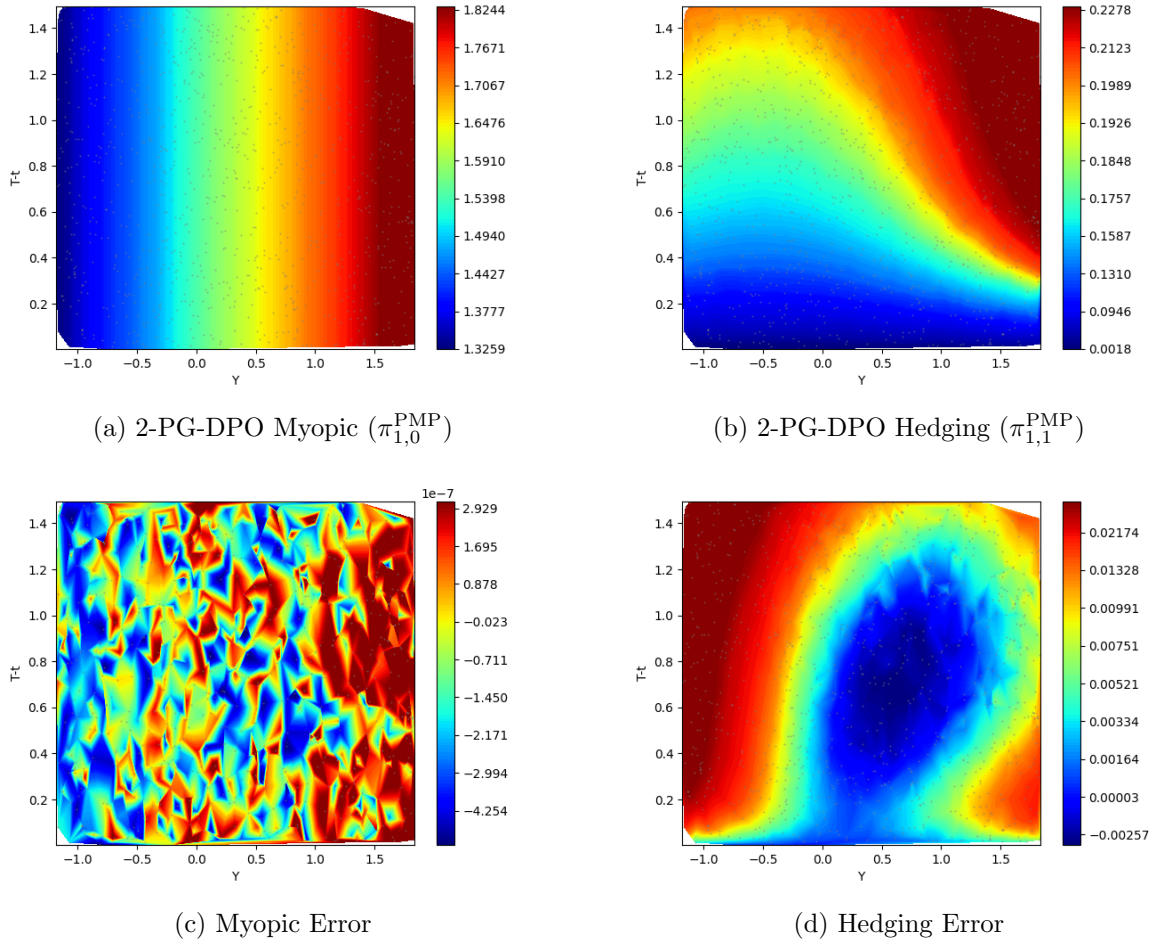


Figure 3: Decomposition of the 2-PG-DPO policy for the first asset ( $i = 1$ ) in the  $n=50, k=10$  case on epoch 3,200 (plotted against  $Y_1$ ). Top row shows myopic and hedging components. Bottom row shows their respective errors (using Symlog scale). Note the use of different color bar ranges, necessary to visualize both the negligible myopic error and the larger hedging error, which dictates the total policy error.

faced with the combined complexity of 50 assets and 10 state variables.

In dramatic contrast, the 2-PG-DPO method provides a highly accurate solution, as shown by its policy (b) and error (d). Comparing the value ranges indicated by the color bars, the error magnitude for the 2-PG-DPO policy is roughly an order of magnitude smaller than the Baseline error, underscoring the robustness and practical necessity of the 2-PG-DPO approach. Although perfect accuracy might be harder to achieve as dimensionality increases (the minimum RMSE of  $1.32 \times 10^{-2}$  is higher than in lower-dimensional cases), it remains remarkably effective and vastly superior to the direct policy learning method.

The component decomposition in Figure 3 confirms the patterns observed previously. The myopic component (a) largely dictates the policy shape, and its associated error (c) remains negligible (confirming quantitative findings that this error is often  $O(10^{-7})$ ), requiring a very small scale on its color bar for visualization. The hedging component (b) contributes visibly to the total policy shape. Crucially, the hedging error (d) is visually almost identical in pattern to the total 2-PG-DPO error (d) when comparing their respective plots, confirming that the overall accuracy is dictated by the precision of estimating the hedging demands.

In conclusion, the  $n = 50, k = 10$  results powerfully demonstrate the capability of the 2-

PG-DPO framework to “break the dimensional barrier”. While the Baseline PG-DPO struggles significantly, 2-PG-DPO delivers a highly accurate and viable solution by leveraging the structure of Pontryagin’s Maximum Principle. Its performance remains remarkably strong and vastly superior to the baseline, solidifying its potential as a practical tool for large-scale, continuous-time portfolio optimization.

## 5 Conclusion

This paper tackled the significant challenge posed by the “curse of dimensionality” in solving large-scale continuous-time portfolio optimization problems. We introduced and developed the Pontryagin-Guided Direct Policy Optimization (PG-DPO) framework, which uniquely combines the theoretical rigor of Pontryagin’s Maximum Principle (PMP) with the power of deep learning, specifically using backpropagation-through-time (BPTT) applied to policy networks representing investment and consumption strategies.

A central contribution is the development of a highly effective “Two-Stage” PG-DPO variant. This method leverages the insight that BPTT applied to simulation paths can yield stable estimates of the crucial Pontryagin costates (and their derivatives) relatively quickly, often much faster than the full policy network converges. By utilizing these rapidly obtained costate estimates within the analytical first-order optimality conditions derived from PMP, the Two-Stage approach efficiently constructs near-optimal control policies, effectively decoupling the estimation of marginal value sensitivities from the full policy optimization.

Our numerical experiments, conducted on a multi-asset, multi-factor affine model chosen for its tractability allowing rigorous benchmark comparisons, demonstrated the practical effectiveness and scalability of this approach. The results consistently showed that the 2-PG-DPO method achieves substantially higher accuracy and faster convergence compared to the baseline end-to-end policy learning strategy. Notably, the framework successfully scaled to problems involving dimensions (e.g.,  $n=50$  assets,  $k=10$  state factors) that are typically considered intractable for traditional numerical HJB/PDE solvers, thereby effectively “breaking the dimensional barrier.” We specifically highlighted the method’s capability to accurately capture both myopic and complex intertemporal hedging demands by explicitly leveraging the structure inherent in the PMP optimality conditions.

While demonstrated on an affine model, the underlying principles relying on PMP and BPTT suggest broader applicability. This research opens several avenues for future investigation. Firstly, further exploration of the theoretical underpinnings is crucial. Our analysis, related to Proposition 3.1, indicates that the rationale behind 2-PG-DPO—leveraging the stability of value function derivatives—is theoretically supported for potentially broad classes of models, possibly including non-affine cases, provided certain **regularity conditions** related to smoothness and parabolicity are met. A key avenue for future theoretical research is to rigorously characterize the precise range of financial models (both affine and non-affine) that satisfy these sufficient regularity assumptions, thereby ensuring the well-posedness of the PMP framework and the reliability of BPTT-based estimates. Furthermore, investigating the general theoretical convergence properties of the PG-DPO algorithm, particularly the costate estimation process, remains an important open question.

Secondly, extending the framework to incorporate more realistic market features is a natural next step for enhancing practical relevance. This includes adapting PG-DPO to handle **portfolio constraints** (like short-selling restrictions or leverage limits) and modeling market frictions such as **transaction costs**, both of which significantly alter the optimal control landscape. Testing the framework’s robustness and performance with **different utility functions** beyond CRRA (e.g., HARA, prospect theory) is also warranted. Moreover, explicitly including the optimization and evaluation of the **intermediate consumption policy**, omitted in the current study for benchmarking clarity, would provide a more complete assessment of the full

framework’s capabilities.

Thirdly, further empirical validation and algorithmic refinements are desirable. Building on the theoretical potential for broader applicability, applying the PG-DPO framework (especially the superior 2-PG-DPO variant) to well-known **non-affine financial models** (e.g., stochastic volatility models like Heston) would be valuable, even in the absence of exact benchmarks, to showcase its capabilities more broadly. Algorithmically, exploring alternative **neural network architectures, advanced optimization techniques, and variance reduction methods** beyond antithetic variates could potentially lead to further performance improvements or faster convergence.

Finally, optimizing the implementation details deserves attention. This includes refining strategies for determining the optimal warm-up duration for the 2-PG-DPO method to best balance costate accuracy against potential overfitting to simulation artifacts inherent in the discrete-time training process. Careful tuning of hyperparameters related to both the network training and the costate estimation phase will be important for practical applications.

## Acknowledgments

This work was supported by the National Research Foundation of Korea (NRF) grant funded by the Korea government (MSIT) (RS-2025-00562904).

## References

- Adams, R. A. & Fournier, J. J. (2003). *Sobolev spaces*, volume 140. Elsevier. (A2)
- Balduzzi, P. & Lynch, A. W. (1999). Transaction costs and predictability: Some utility cost calculations. *Journal of Financial Economics*, 52(1), 47–78. 1
- Bellman, R. (1966). Dynamic programming. *science*, 153(3731), 34–37. 1
- Bertsekas, D. P. & Tsitsiklis, J. N. (1995). Neuro-dynamic programming: an overview. In *Proceedings of 1995 34th IEEE conference on decision and control*, volume 1 (pp. 560–564).: IEEE. 1
- Borkar, V. S. & Borkar, V. S. (2008). *Stochastic approximation: a dynamical systems viewpoint*, volume 9. Springer. 1
- Brandt, M. W., Goyal, A., Santa-Clara, P., & Stroud, J. R. (2005). A simulation approach to dynamic portfolio choice with an application to learning about return predictability. *The Review of Financial Studies*, 18(3), 831–873. 1
- Campbell, J. Y., Chan, Y. L., & Viceira, L. M. (2003). A multivariate model of strategic asset allocation. *Journal of financial economics*, 67(1), 41–80. 1
- Campbell, J. Y. & Viceira, L. M. (1999). Consumption and portfolio decisions when expected returns are time varying. *The Quarterly Journal of Economics*, 114(2), 433–495. 1
- Duarte, V., Duarte, D., & Silva, D. H. (2024). Machine learning for continuous-time finance. *The Review of Financial Studies*, 37(11), 3217–3271. 1
- Evans, L. C. (2022). *Partial differential equations*, volume 19. American Mathematical Society. 3.3.1, 3.3.2, (A2), 3.1, 3.3.2
- Fleming, W. H. & Soner, H. M. (2006). *Controlled Markov processes and viscosity solutions*, volume 25. Springer Science & Business Media. 3.3.1, 3.3.2

- Garlappi, L. & Skoulakis, G. (2010). Solving consumption and portfolio choice problems: The state variable decomposition method. *The Review of Financial Studies*, 23(9), 3346–3400. 1
- Goodfellow, I. (2016). Deep learning. 3.3.3
- Han, J., Jentzen, A., & E, W. (2018). Solving high-dimensional partial differential equations using deep learning. *Proceedings of the National Academy of Sciences*, 115(34), 8505–8510. 1
- Hörmander, L. (1967). Hypoelliptic second order differential equations. 3.3.2
- Huh, J. (2024). A pontryagin-guided neural policy optimization framework for merton’s portfolio problem. *arXiv preprint arXiv:2412.13101*. 1, 3.1
- Karatzas, I., Lehoczky, J. P., & Shreve, S. E. (1987). Optimal portfolio and consumption decisions for a ”small investor” on a finite horizon. *SIAM journal on control and optimization*, 25(6), 1557–1586. 1
- Kim, T. S. & Omberg, E. (1996). Dynamic nonmyopic portfolio behavior. *The Review of Financial Studies*, 9(1), 141–161. 2, 2.3.1, B.1
- Krylov, N. V. (2024). *Lectures on elliptic and parabolic equations in Sobolev spaces*, volume 96. American Mathematical Society. 3.3.2
- Kushner, H. J. & Yin, G. G. (2003). *Stochastic Approximation and Recursive Algorithms and Applications*. New York: Springer Science & Business Media. 1
- Liu, J. (2007). Portfolio selection in stochastic environments. *The Review of Financial Studies*, 20(1), 1–39. 2
- Lynch, A. W. (2001). Portfolio choice and equity characteristics: Characterizing the hedging demands induced by return predictability. *Journal of Financial Economics*, 62(1), 67–130. 1
- Merton, R. C. (1971). Optimum consumption and portfolio rules in a continuous-time model. *Journal of Economic Theory*, 3(4), 373–413. 1, 2
- Nguwi, J. Y., Penent, G., & Privault, N. (2024). A deep branching solver for fully nonlinear partial differential equations. *Journal of Computational Physics*, 499, 112712. 1
- Oksendal, B. (2013). *Stochastic differential equations: an introduction with applications*. Springer Science & Business Media. 2.1, 2.1
- Oleinik, O. (2012). *Second-order equations with nonnegative characteristic form*. Springer Science & Business Media. 3.3.2
- Pennacchi, G. G. (2008). *Theory of asset pricing*. Pearson/Addison-Wesley Boston. 2.1
- Pontryagin, L. S. (2014). *Ordinary Differential Equations: Adiwes International Series in Mathematics*. Elsevier. 1, 2, 3.3.2, 3.3.3
- Raissi, M., Perdikaris, P., & Karniadakis, G. E. (2019). Physics-informed neural networks: A deep learning framework for solving forward and inverse problems involving nonlinear partial differential equations. *Journal of Computational physics*, 378, 686–707. 1
- Yong, J. & Zhou, X. Y. (2012). *Stochastic controls: Hamiltonian systems and HJB equations*, volume 43. Springer Science & Business Media. 1, 2, 2.2, (a), 3.3.1, 3.3.2, 3.3.3

## A Derivation of the Adjoint Diffusion Coefficient via Itô's Lemma

In the Pontryagin framework, the adjoint (or costate) process associated with the investor's wealth  $X_t$  is identified with the partial derivative of the value function  $V$ . Concretely, we set  $\lambda_t = V_X(t, X_t, \mathbf{Y}_t)$ , where  $\mathbf{Y}_t \in \mathbb{R}^k$  represents additional state variables and  $X_t$  is the investor's scalar wealth process. Our goal in this section is to derive the diffusion coefficient corresponding to the  $d\mathbf{W}_t^X$  term in the backward SDE for  $\lambda_t$ , namely  $\mathbf{Z}_t^{\lambda X}$  from BSDE (5), which plays a crucial role in determining the optimal portfolio via FOC (9).

Recall that under an optimal control  $(\boldsymbol{\pi}_t^*, C_t^*)$ , the wealth  $X_t^*$  evolves according to Eq. (3) and Eq. (4), and the  $k$ -dimensional state process  $\mathbf{Y}_t^*$  follows its own SDE, also presented in Section 2.2. The dynamics are driven by correlated Brownian motions  $\mathbf{W}_t^X \in \mathbb{R}^n$  and  $\mathbf{W}_t^Y \in \mathbb{R}^k$  with the joint covariance structure  $\text{Cov}(d\mathbf{W}_t) = \begin{pmatrix} \Psi & \rho \\ \rho^\top & \Phi \end{pmatrix} dt$ .

Since  $\lambda_t = V_X(t, X_t, \mathbf{Y}_t)$ , we apply Ito's multidimensional lemma to  $V_X$ . The differential  $d\lambda_t$  can be expressed as:

$$\begin{aligned} d\lambda_t &= V_{Xt} dt + V_{XX} dX_t + V_{X\mathbf{Y}} d\mathbf{Y}_t \\ &\quad + \frac{1}{2} V_{XXX} (dX_t)^2 + V_{XX\mathbf{Y}} (dX_t) (d\mathbf{Y}_t)^\top + \frac{1}{2} \text{Tr}(V_{X\mathbf{Y}\mathbf{Y}} (d\mathbf{Y}_t)(d\mathbf{Y}_t)^\top), \end{aligned} \quad (19)$$

where subscripts denote partial derivatives (e.g.,  $V_{X\mathbf{Y}}$  is the gradient w.r.t  $\mathbf{Y}$  of  $V_X$ ,  $V_{X\mathbf{Y}\mathbf{Y}}$  is the Hessian w.r.t  $\mathbf{Y}$  of  $V_X$ ).

Our objective is to identify the coefficient of  $d\mathbf{W}_t^X$  in the expansion of  $d\lambda_t$ . This coefficient is precisely the process  $\mathbf{Z}_t^{\lambda X}$  appearing in the BSDE (5). Substituting the SDEs for  $dX_t$  and  $d\mathbf{Y}_t$  (from Section 2.2) into the Ito formula (19), we observe that terms involving  $d\mathbf{W}_t^X$  arise directly from the diffusion part of the  $V_{XX} dX_t$  term, and indirectly from the  $V_{X\mathbf{Y}} d\mathbf{Y}_t$  term due to the correlation  $\rho$  between  $d\mathbf{W}_t^X$  and  $d\mathbf{W}_t^Y$ . A careful application of Ito's lemma, considering the quadratic variation and covariation terms related to the covariance matrix  $\begin{pmatrix} \Psi & \rho \\ \rho^\top & \Phi \end{pmatrix}$ , allows isolation of the full coefficient multiplying  $d\mathbf{W}_t^X$ . Representing  $\mathbf{Z}_t^{\lambda X}$  as a  $1 \times n$  row vector, this process is found to be:

$$\mathbf{Z}_t^{\lambda X} = \underbrace{(\partial_x \lambda_t^*) X_t^* \boldsymbol{\pi}_t^{*\top} \boldsymbol{\sigma}(t, \mathbf{Y}_t^*)}_{\text{Term from } V_{XX} dX_t} + \underbrace{(\partial_{\mathbf{Y}} \lambda_t^*) \boldsymbol{\sigma}_Y(t, \mathbf{Y}_t^*) \rho^\top \Psi^{-1}}_{\text{Term from } V_{X\mathbf{Y}} d\mathbf{Y}_t \text{ via correlation}}. \quad (20)$$

The first term reflects the direct impact of wealth volatility related to the portfolio choice  $\boldsymbol{\pi}_t^*$ , scaled by the second derivative of the value function with respect to wealth,  $V_{XX}$  (or  $\partial_x \lambda_t^*$ ). The second term captures the intertemporal hedging component arising from the correlation between asset returns and state variable movements, mediated by the cross-derivative of the value function  $V_{X\mathbf{Y}}$  (or  $\partial_{\mathbf{Y}} \lambda_t^*$ ).

This derivation provides the explicit form of the adjoint diffusion coefficient  $\mathbf{Z}_t^{\lambda X}$ , which is fundamental for understanding the structure of the optimal portfolio policy (10) and for constructing the Pontryagin adjoint equations.

## B Analytic Solutions for Affine Models

This appendix provides details on the derivation of analytic solutions for the portfolio optimization problems presented in Section 2.3 under specific assumptions (no intermediate consumption, CRRA utility), typically following the Hamilton-Jacobi-Bellman (HJB) approach with an exponential-quadratic value function ansatz. We also show how these solutions connect to the Pontryagin framework.

## B.1 Analytic Solution for the Multi-Asset OU Model (Section 2.3.1)

For simplicity, we assume no intermediate consumption, i.e.,  $C_t = 0$ , and consider an investor who derives utility only from terminal wealth  $X_T$  under a CRRA objective  $U(x) = \frac{x^{1-\gamma}}{1-\gamma}$ . Following Kim & Omberg (1996), the associated Hamilton–Jacobi–Bellman (HJB) equation can be solved by positing a value function of the form:

$$V(t, x, Y) = \frac{x^{1-\gamma}}{1-\gamma} \exp\left(g(t) + B(t)Y + \frac{1}{2}C(t)Y^2\right). \quad (21)$$

Here,  $g(t)$ ,  $B(t)$ , and  $C(t)$  are deterministic functions of time determined by solving a system of ordinary differential equations (ODEs) derived from the HJB equation, subject to terminal conditions at  $t = T$ .

From this value function, the costate  $\lambda_t^* = V_x$ , its derivative with respect to wealth  $\partial_x \lambda_t^* = V_{xx}$ , and its derivative with respect to the state  $\partial_Y \lambda_t^* = V_{xY}$  have the following closed-form expressions on the optimal path  $(X_t^*, Y_t)$ :

$$\begin{aligned} \lambda_t^*(t, X_t^*, Y_t) &= (X_t^*)^{-\gamma} \exp\left(g(t) + B(t)Y_t + \frac{1}{2}C(t)Y_t^2\right), \\ \frac{\partial \lambda_t^*}{\partial x}(t, X_t^*, Y_t) &= -\gamma (X_t^*)^{-\gamma-1} \exp\left(g(t) + B(t)Y_t + \frac{1}{2}C(t)Y_t^2\right), \\ \frac{\partial \lambda_t^*}{\partial Y}(t, X_t^*, Y_t) &= (X_t^*)^{-\gamma} (B(t) + C(t)Y_t) \exp\left(g(t) + B(t)Y_t + \frac{1}{2}C(t)Y_t^2\right). \end{aligned}$$

These expressions lead to remarkably simple ratios that are central to the Pontryagin framework's characterization of the optimal portfolio:

$$\frac{\lambda_t^*}{\partial_x \lambda_t^*} = -\frac{X_t^*}{\gamma}, \quad \frac{\partial_Y \lambda_t^*}{\partial_x \lambda_t^*} = -\frac{X_t^*}{\gamma} (B(t) + C(t)Y_t).$$

Substituting these ratios into the general Pontryagin first-order condition for the optimal portfolio  $\pi_t^*$  (which equates the marginal contribution to the Hamiltonian from investing in risky assets to zero, cf. Eq. (9) derived in Section 2.2) confirms the explicit analytic solution derived via the HJB approach:

$$\pi^*(t, Y) = \frac{1}{\gamma} \Sigma^{-1} \left[ \underbrace{(\boldsymbol{\alpha} \boldsymbol{\sigma}) Y}_{\text{Myopic}} + \underbrace{\sigma_Y (\boldsymbol{\sigma} \boldsymbol{\rho}) (B(t) + C(t) Y)}_{\text{Hedging}} \right],$$

where  $\Sigma = \text{diag}(\boldsymbol{\sigma}) \Psi \text{diag}(\boldsymbol{\sigma})$ ,  $\boldsymbol{\alpha} = (\alpha_1, \dots, \alpha_n)^\top$ ,  $\boldsymbol{\rho} = (\rho_1, \dots, \rho_n)^\top$ ,  $(\boldsymbol{\alpha} \boldsymbol{\sigma})$  is the vector  $(\alpha_1 \sigma_1, \dots, \alpha_n \sigma_n)^\top$ , and  $(\boldsymbol{\sigma} \boldsymbol{\rho})$  is the vector  $(\sigma_1 \rho_1, \dots, \sigma_n \rho_n)^\top$ . The derivation confirms that the first term captures the myopic demand driven by the instantaneous risk premium  $(\boldsymbol{\mu}(Y) - r\mathbf{1}) = (\boldsymbol{\alpha} \boldsymbol{\sigma}) Y$ , while the second term represents the intertemporal hedging demand, proportional to  $B(t) + C(t)Y$  which arises from the state-dependency of the investment opportunity set captured by  $\partial_Y \lambda_t^*$ .

Substituting this  $\pi^*$  back into the HJB equation and matching coefficients in powers of  $Y$  yields the following Riccati-type ODEs for  $B(t)$  and  $C(t)$ , along with the ODE for  $g(t)$ . The system is solved backward from the terminal conditions:

$$g(T) = 0, \quad B(T) = 0, \quad C(T) = 0. \quad (22)$$

The ODEs are:

$$-\frac{dC(t)}{dt} = -2\kappa_Y C(t) + \sigma_Y^2 C(t)^2 + \frac{1-\gamma}{\gamma} \left[ \beta_0 + 2\sigma_Y C(t) \beta_1 + \sigma_Y^2 C(t)^2 \beta_2 \right], \quad (23)$$

$$-\frac{dB(t)}{dt} = -\kappa_Y B(t) + \sigma_Y^2 B(t) C(t) - \frac{1-\gamma}{\gamma} \left[ \sigma_Y^2 B(t) C(t) \beta_2 + \sigma_Y B(t) \beta_1 \right] + \kappa_Y \theta_Y C(t), \quad (24)$$

$$\frac{dg(t)}{dt} = (1-\gamma)r - \frac{1-\gamma}{2\gamma} \left[ \beta_0 + 2\sigma_Y \beta_1 B(t) + \sigma_Y^2 \beta_2 (B(t)^2 + C(t)) \right] + \kappa_Y \theta_Y B(t) + \frac{1}{2} \sigma_Y^2 C(t). \quad (25)$$

Here,  $r$  is the risk-free rate,  $\kappa_Y$ ,  $\theta_Y$ ,  $\sigma_Y$  are the OU parameters,  $\gamma$  is the risk aversion coefficient, and  $\beta_0$ ,  $\beta_1$ ,  $\beta_2$  are quadratic forms involving the model parameters defined as:

$$\beta_0 := (\boldsymbol{\alpha} \boldsymbol{\sigma})^\top \Sigma^{-1} (\boldsymbol{\alpha} \boldsymbol{\sigma}), \quad \beta_1 := (\boldsymbol{\alpha} \boldsymbol{\sigma})^\top \Sigma^{-1} (\boldsymbol{\sigma} \boldsymbol{\rho}), \quad \beta_2 := (\boldsymbol{\sigma} \boldsymbol{\rho})^\top \Sigma^{-1} (\boldsymbol{\sigma} \boldsymbol{\rho}).$$

By solving the system of ODEs (23), (24), and (25) backward in time from the terminal conditions (22), one obtains the functions  $g(t)$ ,  $B(t)$ , and  $C(t)$ . Substituting these into Eq. (21) gives the complete analytic form of the value function consistent with the underlying HJB/PMP framework.

## B.2 Analytic Solution for the Multi-Asset Multi-Factor Model (Section 2.3.2)

For simplicity, we again assume no intermediate consumption ( $C_t = 0$ ) and focus on an investor who maximizes the expected utility of terminal wealth under CRRA utility  $U(x) = \frac{x^{1-\gamma}}{1-\gamma}$ . Following related literature on multi-factor affine models, we posit a value function of the form

$$V(t, x, \mathbf{Y}) = \frac{x^{1-\gamma}}{1-\gamma} \exp \left\{ g(t) + \mathbf{B}(t)^\top \mathbf{Y} + \frac{1}{2} \mathbf{Y}^\top \mathbf{C}(t) \mathbf{Y} \right\}, \quad (26)$$

where  $\mathbf{B}(t)$  is an  $k \times 1$  vector,  $\mathbf{C}(t)$  is an  $k \times k$  symmetric matrix (note: dimensions based on state vector  $\mathbf{Y} \in \mathbb{R}^k$ ), and  $g(t)$  is a scalar function, all satisfying ODEs derived from the HJB equation, with terminal conditions  $g(T) = 0$ ,  $\mathbf{B}(T) = \mathbf{0}$  and  $\mathbf{C}(T) = \mathbf{0}$ .

Define the relevant matrices and vectors:

$$\boldsymbol{\sigma} = \text{diag}(\sigma_1, \dots, \sigma_n), \quad \boldsymbol{\sigma}_Y \text{ (factor diffusion } k \times k), \quad \Sigma = \boldsymbol{\sigma} \Psi \boldsymbol{\sigma}.$$

where  $\Psi \in \mathbb{R}^{n \times n}$  is the correlation matrix for the  $n$  risky assets, and let  $\boldsymbol{\rho} \in \mathbb{R}^{n \times k}$  be the cross-correlation matrix between these assets and the  $k$ -dimensional factor Brownian motion  $\mathbf{W}_t^Y$ . Also let  $\mathbf{A} = (\boldsymbol{\alpha}_1, \dots, \boldsymbol{\alpha}_n)^\top \in \mathbb{R}^{n \times k}$  collect the factor loadings  $\boldsymbol{\alpha}_i \in \mathbb{R}^k$  for each asset  $i$ .

The costate  $\lambda_t^* = V_x$ , its derivative with respect to wealth  $\partial_x \lambda_t^* = V_{xx}$ , and its gradient ( $k \times 1$  vector) with respect to the state vector  $\partial_{\mathbf{Y}} \lambda_t^* = V_{x\mathbf{Y}}$  are given by:

$$\begin{aligned} \lambda_t^*(t, X_t^*, \mathbf{Y}_t) &= (X_t^*)^{-\gamma} \exp \left( g(t) + \mathbf{B}(t)^\top \mathbf{Y}_t + \frac{1}{2} \mathbf{Y}_t^\top \mathbf{C}(t) \mathbf{Y}_t \right), \\ \frac{\partial \lambda_t^*}{\partial x}(t, X_t^*, \mathbf{Y}_t) &= -\gamma (X_t^*)^{-\gamma-1} \exp \left( g(t) + \mathbf{B}(t)^\top \mathbf{Y}_t + \frac{1}{2} \mathbf{Y}_t^\top \mathbf{C}(t) \mathbf{Y}_t \right), \\ \frac{\partial \lambda_t^*}{\partial \mathbf{Y}}(t, X_t^*, \mathbf{Y}_t) &= (X_t^*)^{-\gamma} (\mathbf{B}(t) + \mathbf{C}(t) \mathbf{Y}_t) \exp \left( g(t) + \mathbf{B}(t)^\top \mathbf{Y}_t + \frac{1}{2} \mathbf{Y}_t^\top \mathbf{C}(t) \mathbf{Y}_t \right). \end{aligned}$$

These yield the following scalar and vector ratios, which simplify the PMP optimality conditions:

$$\frac{\lambda_t^*}{\partial_x \lambda_t^*} = -\frac{X_t^*}{\gamma}, \quad \frac{\partial_{\mathbf{Y}} \lambda_t^*}{\partial_x \lambda_t^*} = -\frac{X_t^*}{\gamma} (\mathbf{B}(t) + \mathbf{C}(t) \mathbf{Y}_t).$$

Substituting these into the vector form of the PMP first-order condition for the optimal portfolio  $\boldsymbol{\pi}_t^* \in \mathbb{R}^n$ , (cf. Eq. (10) derived in Section 2.2):

$$\boldsymbol{\pi}_t^* = -\frac{1}{X_t^* \partial_x \lambda_t^*} \Sigma^{-1} \left\{ \lambda_t^* (\boldsymbol{\mu}(\mathbf{Y}_t) - r\mathbf{1}) + \boldsymbol{\sigma} \boldsymbol{\rho} \boldsymbol{\sigma}_Y \left[ (\partial_{\mathbf{Y}} \lambda_t^*)^\top \right] \right\},$$

where the risk premium vector is  $\boldsymbol{\mu}(\mathbf{Y}_t) - r\mathbf{1} = \boldsymbol{\sigma} \mathbf{A} \mathbf{Y}_t$ , we precisely recover the analytic solution obtained from the HJB framework:

$$\boldsymbol{\pi}^*(t, \mathbf{Y}) = \frac{1}{\gamma} \Sigma^{-1} \left[ \underbrace{\boldsymbol{\sigma} \mathbf{A} \mathbf{Y}}_{\text{Myopic component (related to } \boldsymbol{\mu} - r\mathbf{1})} + \underbrace{\boldsymbol{\sigma} \boldsymbol{\rho} \boldsymbol{\sigma}_Y (\mathbf{B}(t) + \mathbf{C}(t) \mathbf{Y})}_{\text{Hedging component (related to } \partial_{\mathbf{Y}} \lambda_t^*)} \right].$$

Here, the first bracketed term corresponds to the *myopic* component, driven by the instantaneous expected excess returns  $\boldsymbol{\sigma} \mathbf{A} \mathbf{Y}$ . The second bracketed term incorporates *intertemporal hedging* demands arising from the desire to hedge against unfavorable changes in the investment opportunity set, as captured by the factor sensitivities  $\mathbf{B}(t) + \mathbf{C}(t)\mathbf{Y}$  (proportional to the gradient  $\partial_{\mathbf{Y}} \lambda_t^*$ ) and the correlations encoded in  $\rho$ ,  $\Psi$ , and  $\Phi$  (implicitly via the ODEs for  $\mathbf{B}$  and  $\mathbf{C}$ ).

To determine the time-dependent coefficients  $\mathbf{B}(t)$  and  $\mathbf{C}(t)$ , we solve the backward matrix Riccati ODE system derived from substituting the value function ansatz and optimal portfolio into the HJB equation:

$$\begin{aligned} \frac{d\mathbf{C}(t)}{dt} &= \kappa_Y^\top \mathbf{C}(t) + \mathbf{C}(t) \kappa_Y - \mathbf{C}(t) \boldsymbol{\sigma}_Y \Phi \boldsymbol{\sigma}_Y^\top \mathbf{C}(t) \\ &\quad - \frac{1-\gamma}{\gamma} \left[ (\mathbf{A}^\top \boldsymbol{\sigma}) \Sigma^{-1} (\boldsymbol{\sigma} \mathbf{A}) + (\mathbf{A}^\top \boldsymbol{\sigma}) \Sigma^{-1} (\boldsymbol{\sigma} \rho \boldsymbol{\sigma}_Y) \mathbf{C}(t) \right. \\ &\quad \left. + \mathbf{C}(t) (\boldsymbol{\sigma}_Y^\top \rho^\top \boldsymbol{\sigma}) \Sigma^{-1} (\boldsymbol{\sigma} \mathbf{A}) + \mathbf{C}(t) (\boldsymbol{\sigma}_Y^\top \rho^\top \boldsymbol{\sigma}) \Sigma^{-1} (\boldsymbol{\sigma} \rho \boldsymbol{\sigma}_Y) \mathbf{C}(t) \right], \end{aligned} \quad (27)$$

$$\begin{aligned} \frac{d\mathbf{B}(t)}{dt} &= \left[ \kappa_Y^\top - \mathbf{C}(t) \boldsymbol{\sigma}_Y \Phi \boldsymbol{\sigma}_Y^\top - \frac{1-\gamma}{\gamma} \left( \mathbf{C}(t) (\boldsymbol{\sigma}_Y^\top \rho^\top \boldsymbol{\sigma}) \Sigma^{-1} (\boldsymbol{\sigma} \rho \boldsymbol{\sigma}_Y) + (\mathbf{A}^\top \boldsymbol{\sigma}) \Sigma^{-1} (\boldsymbol{\sigma} \rho \boldsymbol{\sigma}_Y) \right) \right] \mathbf{B}(t) \\ &\quad - \left[ \mathbf{C}(t) \kappa_Y - \frac{1-\gamma}{\gamma} (\mathbf{A}^\top \boldsymbol{\sigma}) \Sigma^{-1} (\boldsymbol{\sigma} \mathbf{A}) \right] \boldsymbol{\theta}_Y. \end{aligned} \quad (28)$$

subject to the terminal conditions  $\mathbf{C}(T) = \mathbf{0}$  and  $\mathbf{B}(T) = \mathbf{0}$ .

To obtain the complete value function (26), the scalar function  $g(t)$  must also be determined by solving its own ODE backward from the terminal condition  $g(T) = 0$ . This ODE, derived from the HJB equation by collecting terms independent of  $\mathbf{Y}$  and consistent with the corrected single-factor case structure, is given by:

$$\begin{aligned} \frac{dg(t)}{dt} &= (1-\gamma)r \\ &\quad - \frac{1-\gamma}{2\gamma} \text{Tr} \left( (\mathbf{A}^\top \boldsymbol{\sigma}) \Sigma^{-1} (\boldsymbol{\sigma} \mathbf{A}) \right) \\ &\quad - \frac{1-\gamma}{\gamma} \mathbf{B}(t)^\top (\boldsymbol{\sigma}_Y^\top \rho^\top \boldsymbol{\sigma}) \Sigma^{-1} (\boldsymbol{\sigma} \mathbf{A}) \\ &\quad - \frac{1-\gamma}{2\gamma} \left[ \mathbf{B}(t)^\top (\boldsymbol{\sigma}_Y^\top \rho^\top \boldsymbol{\sigma}) \Sigma^{-1} \boldsymbol{\sigma} \rho \boldsymbol{\sigma}_Y \mathbf{B}(t) + \text{Tr} \left( (\boldsymbol{\sigma}_Y^\top \rho^\top \boldsymbol{\sigma}) \Sigma^{-1} \boldsymbol{\sigma} \rho \boldsymbol{\sigma}_Y \mathbf{C}(t) \right) \right] \\ &\quad + \mathbf{B}(t)^\top \kappa_Y \boldsymbol{\theta}_Y \\ &\quad + \frac{1}{2} \text{Tr}(\mathbf{C}(t) \boldsymbol{\sigma}_Y \Phi \boldsymbol{\sigma}_Y^\top). \end{aligned} \quad (29)$$

Here,  $\Phi = \text{Cov}(d\mathbf{W}_t^Y)/dt$  is the factor covariance matrix used in the factor dynamics  $d\mathbf{Y}_t$ , and  $\text{Tr}(\cdot)$  denotes the trace of a matrix.

Solving these coupled ODEs for  $\mathbf{C}(t)$ ,  $\mathbf{B}(t)$ , and  $g(t)$  backward in time from  $T$  to  $t$  and substituting the results into Eq. (26) gives the closed-form value function, while substituting  $\mathbf{B}(t)$  and  $\mathbf{C}(t)$  into  $\boldsymbol{\pi}^*(t, \mathbf{Y})$  gives the optimal strategy, explicitly capturing both *myopic* and *intertemporal hedging* components in a multi-asset, multi-factor setting.

## C Detailed Experimental Setup

This appendix provides the detailed setup for the numerical experiments presented in Section 4.

### C.1 Parameter Values

The experiments consider the objective of maximizing the expected utility of terminal wealth  $X_T$ ,  $J = \mathbb{E}[U(X_T)]$ , using a CRRA utility function  $U(x) = x^{1-\gamma}/(1-\gamma)$  with a relative risk

aversion coefficient  $\gamma = 2.0$ . The fixed time horizon is  $T = 1.5$ .

Unless otherwise specified, the model parameters (for the model described in Section 2.3.2) are generated based on the asset dimension  $n$  and factor dimension  $k$  using the following process (seeded for reproducibility, e.g., ‘seed=42’):

- Risk-free rate:  $r = 0.03$ .
- State process parameters (for the  $k$ -dimensional OU process  $\mathbf{Y}_t$ ):
  - Mean-reversion speeds:  $\boldsymbol{\kappa}_Y = \text{diag}(2.0, 2.5, \dots, 2.0 + (k - 1)0.5)$ .
  - Long-term means:  $\boldsymbol{\theta}_Y$  components drawn uniformly from  $U(0.2, 0.4)$ .
  - Factor volatilities:  $\boldsymbol{\sigma}_Y$  diagonal elements drawn uniformly from  $U(0.3, 0.5)$ .
- Asset parameters (for the  $n$  risky assets):
  - Volatilities:  $\boldsymbol{\sigma} \in \mathbb{R}^n$  components drawn uniformly from  $U(0.1, 0.5)$ .
  - Factor loadings ( $\boldsymbol{\alpha} \in \mathbb{R}^{n \times k}$ ): For each asset  $i = 1, \dots, n$ , the  $k$ -dimensional row vector of factor loadings  $\boldsymbol{\alpha}_i^\top = (\alpha_{i1}, \dots, \alpha_{ik})$  is drawn independently from a Dirichlet distribution. This is done using ‘scipy.stats.dirichlet’ with a concentration parameter vector consisting of  $k$  ones ( $\mathbf{1}_k = [1.0, \dots, 1.0]$ ). Consequently, for each asset  $i$ , all loadings are non-negative ( $\alpha_{ij} \geq 0$ ) and they sum to unity ( $\sum_{j=1}^k \alpha_{ij} = 1$ ). (Note: These loadings define the risk premium structure  $\boldsymbol{\mu}(t, \mathbf{Y}_t) = r\mathbf{1} + \text{diag}(\boldsymbol{\sigma})\boldsymbol{\alpha}\mathbf{Y}_t$ ).
- Correlation structure: The generation process aims to produce realistic correlation parameters while ensuring the overall block correlation matrix remains positive definite, which is crucial for stable simulations. This involves:
  - Asset correlation  $\Psi$  ( $n \times n$ ) generated based on a latent factor structure ensuring validity.
  - Factor correlation  $\Phi_Y$  ( $k \times k$ ) generated as a random correlation matrix.
  - Cross-correlation  $\boldsymbol{\rho}_Y$  ( $n \times k$ ) components drawn uniformly from  $U(-0.2, 0.2)$ .
  - The full  $(n + k) \times (n + k)$  block correlation matrix  $\begin{pmatrix} \Psi & \boldsymbol{\rho}_Y \\ \boldsymbol{\rho}_Y^\top & \Phi_Y \end{pmatrix}$  is constructed and numerically adjusted (e.g., via minimal diagonal loading) if necessary to ensure positive definiteness (tolerance  $10^{-6}$ ).

The specific values generated by the seed are used consistently across experiments for given  $n$  and  $k$ .

## C.2 PG-DPO Implementation Details

We implement the Baseline PG-DPO algorithm using PyTorch.

- **Policy Network ( $\boldsymbol{\pi}_\theta$ ):** The policy network architecture consists of an input layer taking the current wealth  $W_t$ , current time  $t$ , and state vector  $\mathbf{Y}_t$  (total  $2 + k$  inputs), followed by three hidden layers with 200 units each and LeakyReLU activation, and an output layer producing the  $n$ -dimensional portfolio weight vector  $\boldsymbol{\pi}_\theta$ .
- **Optimizer:** Adam optimizer with a learning rate of  $1 \times 10^{-5}$ .
- **Training:**
  - Total epochs: 10,000.
  - Batch size ( $M$ ): 1,000.

- Time discretization steps ( $N$ ): 20.
- Initial state sampling ( $\eta$ ): For each trajectory in a batch, the initial time  $t_0$  is drawn uniformly from  $[0, T)$ , initial wealth  $W_0$  from  $U(0.1, 3.0)$ . The initial state variables  $\mathbf{Y}_0 = (Y_{0,1}, \dots, Y_{0,k})^\top$  are sampled such that each component  $Y_{0,i}$  is drawn independently and uniformly from a single common range  $[Y_{\min}, Y_{\max}]$ . This range is determined by the minimum lower bound and the maximum upper bound observed across all individual factors’ typical  $\pm 3\sigma$  intervals:

$$Y_{\min} = \min_{i=1, \dots, k} (\theta_{Y,i} - 3\sigma_{Y,ii}), \quad Y_{\max} = \max_{i=1, \dots, k} (\theta_{Y,i} + 3\sigma_{Y,ii}),$$

where  $\theta_{Y,i}$  is the long-term mean and  $\sigma_{Y,ii}$  is the instantaneous volatility parameter for the  $i$ -th factor. The simulation then runs forward from  $t_0$  to the fixed horizon  $T$  using  $N = 20$  time steps, with step size  $\Delta t = (T - t_0)/N$ . This approach ensures the policy is trained effectively across the entire time interval  $[0, T]$  and a relevant hypercube in the state space defined by the collective factor dynamics.

- Variance Reduction: Antithetic variates used.
- Wealth constraint: Simulated wealth  $W_t$  clamped at lower bound 0.1.
- **Costate Estimation (for Two-Stage Evaluation):** During periodic evaluation, costate  $\lambda$  and derivatives  $\partial_x \lambda, \partial_{\mathbf{Y}} \lambda$  are computed via BPTT (‘torch. autograd.grad’) applied to Monte Carlo estimates of the expected terminal utility starting from evaluation points  $(t_k, W_k, \mathbf{Y}_k)$ .

### C.3 Benchmark Solution and Evaluation

As mentioned, the chosen multi-factor OU model allows for a semi-analytical benchmark solution. It is important to note that these experiments focus solely on the terminal wealth objective ( $J = \mathbb{E}[U(X_T)]$ ), and thus do not include optimization or a neural network for the consumption policy  $C_\phi$ . This simplification is made specifically to enable direct comparison with the semi-analytical benchmark solution derived from the HJB equation, which is readily available for the terminal wealth problem in this affine setting.

- **Benchmark Computation:** The system of ODEs (including a matrix Riccati equation) associated with the HJB equation for this terminal wealth problem (Appendix B.2) is solved numerically backwards from the fixed horizon  $T$  using ‘scipy.integrate.solve\_ivp’ (‘Radau’ method) to obtain the coefficients determining the value function and the optimal policy  $\pi^*(t, W_t, \mathbf{Y}_t)$ .
- **Interpolation:** The benchmark policy (total, myopic, and hedging components) is pre-computed on a grid over  $(t, W_t, \mathbf{Y}_t)$  space and stored using ‘scipy.interpolate.RegularGridInterpolator’ for efficient lookup.
- **Evaluation Metrics:** Performance is evaluated via the Root Mean Squared Error (RMSE) between the policies generated by (i) Baseline PG-DPO ( $\pi_\theta$ ) and the benchmark ( $\pi^*$ ), and (ii) Two-Stage PG-DPO (using Eq. (10) with BPTT-estimated costates) and the benchmark ( $\pi^*$ ). RMSEs are computed for total, myopic, and hedging components.
- **Visualization:** Contour plots compare the learned policies and the benchmark over the state space (typically time  $t$  vs. one state variable  $Y_k$ ), alongside error plots and costate visualizations.

All computations are performed using PyTorch on an NVIDIA A6000 GPU.